TITLE: Longitudinal Profiling of the Intestinal Microbiome in Children with Cystic Fibrosis Treated with Elexacaftor-Tezacaftor-Ivacaftor

WORD COUNT (MAIN TEXT): 4733

AUTHORS: Seth A. Reasoner[1]*, Rachel Bernard[2]*, Adam Waalkes[3], Kelsi Penewit[3], Janessa Lewis[3], Andrew G. Sokolow[4], Rebekah F. Brown[4], Kathryn M. Edwards[5], Stephen J. Salipante[3], Maria Hadjifrangiskou[1,6,7], Maribeth R. Nicholson[2,7]

AFFILIATIONS:

1. Division of Molecular Pathogenesis, Department of Pathology, Microbiology & Immunology, Vanderbilt University Medical Center, Nashville, TN, USA
2. Division of Gastroenterology, Hepatology, and Nutrition, Department of Pediatrics, Monroe Carrell Junior Children's Hospital at Vanderbilt, Nashville, TN, USA
3. Department of Laboratory Medicine and Pathology, University of Washington, Seattle, WA, USA
4. Division of Allergy, and Immunology, and Pulmonary Medicine, Department of Pediatrics, Monroe Carrell Junior Children's Hospital at Vanderbilt, Nashville, TN, USA
5. Division of Infectious Diseases, Department of Pediatrics, Monroe Carrell Junior Children's Hospital at Vanderbilt, Nashville, Tennessee, USA
6. Center for Personalized Microbiology (CPMi), Vanderbilt University Medical Center, Nashville, TN, USA
7. Vanderbilt Institute for Infection, Immunology and Inflammation, Vanderbilt University Medical Center, Nashville, Tennessee, USA

**These authors contributed equally to this work. Authorship position was determined by relative contributions made to this manuscript's completion.*

Corresponding Author:
Maribeth R. Nicholson, MD, MPH
Monroe Carell Jr. Children's Hospital at Vanderbilt
2200 Children's Way, Nashville, TN 37232
Telephone: +1 615 322 7449
E-mail: maribeth.r.nicholson@vumc.org

RUNNING TITLE: CF Gut Microbiome Following CFTR Modulator ELX/TEZ/IVA

KEY WORDS
Cystic fibrosis; CFTR modulators; microbiome; elexacaftor; ivacaftor; tezacaftor; metagenomic sequencing; intestinal inflammation; antibiotic resistance; pediatric

ABSTRACT

The intestinal microbiome influences growth and disease progression in children with cystic fibrosis (CF). Elexacaftor-tezacaftor-ivacaftor (ELX/TEZ/IVA), the newest pharmaceutical modulator for CF, restores function of the pathogenic mutated CFTR channel. We performed a single-center longitudinal analysis of the effect of ELX/TEZ/IVA on the intestinal microbiome, intestinal inflammation, and clinical parameters in children with CF. Following ELX/TEZ/IVA, children with CF had significant improvements in BMI, ppFEV$_1$ and required fewer antibiotics for respiratory infections. Intestinal microbiome diversity increased following ELX/TEZ/IVA coupled with a decrease in the intestinal carriage of *Staphylococcus aureus*, the predominant respiratory pathogen in children with CF. There was a reduced abundance of microbiome-encoded antibiotic-resistance genes. Microbial pathways for aerobic respiration were reduced after ELX/TEZ/IVA. The abundance of microbial acid tolerance genes was reduced, indicating microbial adaptation to increased CFTR function. In all, this study represents the first comprehensive analysis of the intestinal microbiome in children with CF receiving ELX/TEZ/IVA.

IMPORTANCE

Cystic fibrosis is an autosomal recessive disease with significant gastrointestinal symptoms in addition to pulmonary complications. Prior work has shown that the intestinal microbiome correlates with health outcomes in CF, particularly in children. Recently approved treatments for CF, CFTR modulators, are anticipated to substantially improve the care of patients with CF and extend their lifespans. Here, we study the intestinal microbiome of children with CF before and after the CFTR modulator, ELX/TEZ/IVA. We identify promising improvements in microbiome diversity, reduced measures of intestinal inflammation, and reduced antibiotic resistance genes. We present specific bacterial taxa and protein groups which change following ELX/TEZ/IVA. These results will inform future mechanistic studies to understand the microbial improvements associated with CFTR modulator treatment. This study demonstrates how the microbiome can change in response to a targeted medication that corrects a genetic disease.

1. INTRODUCTION

Cystic fibrosis (CF) is an autosomal recessive disease affecting a total of 40,000 individuals in the United States (1). CF is caused by mutations in the CF transmembrane conductance regulator (*CFTR*) gene resulting in decreased epithelial transport of chloride and bicarbonate ions. These mutations result in mucus obstruction which presents with severe multi-organ dysfunction, principally affecting the airways and gastrointestinal tract (2–5). The gastrointestinal complications include malnutrition, dysmotility, and hepatopancreaticobiliary disease (2). Importantly, nutritional status and intestinal microbiome abnormalities in children with CF have been linked to growth failure, disease progression, and risk of future lung transplantation (6–11).

Multiple studies have demonstrated differences in the intestinal microbiome of patients with CF when compared to healthy controls (8, 12–15). The CF intestinal microbiome is notably inflammatory and associated with higher rates of inflammatory bowel disease (IBD) and colon cancer (16–20). In infants with CF, delayed intestinal microbiome maturation has been shown to influence linear growth and immune programming (8, 21). Among the most striking differences compared to healthy controls is the abundance of Proteobacteria, specifically *Escherichia coli*, and concomitant decrease in Bacteroidetes in infants with CF (8, 12, 22–24). Furthermore, during acute CF pulmonary exacerbations, the intestinal microbiome is distinguishable from periods of respiratory stability (15, 21, 25). Respiratory pathogens, such as *Staphylococcus aureus*, can also be detected in CF stool samples (22, 26).

Over the past decade, small molecule therapies which address the primary defect in the CFTR protein and rescue CFTR function in select genotypes have been developed. These "CFTR modulators" have dramatically changed the trajectory of CF patient care, yielding remarkable improvements in lung function, growth, and projected lifespan (27). The most recent CFTR modulator formulation approved for clinical care, elexacaftor-tezacaftor-ivacaftor (ELX/TEZ/IVA), includes two CFTR correctors (ELX & IVA) and one CFTR potentiator (TEZ) (28). The approval of ELX/TEZ/IVA is anticipated to be the most important advancement in CF therapy since *CFTR* was identified over 30 years ago (27, 28).

Given the progressive nature of CF, initiation of therapy in early childhood is critical to stall disease progression. ELX/TEZ/IVA was approved by the FDA for pediatric patients in 2019 (ages 12 years and older), 2021 (ages 6-11 years old), and 2023 (ages 2-5 years old). The impact of ELX/TEZ/IVA on clinical outcomes and the intestinal microbiome in children with CF requires targeted study. To date, studies examining the effects of CFTR modulators on the intestinal microbiome have been limited by the use of single modulator formulations or small

cohort sizes (29–31). Importantly, no studies have characterized the effect of ELX/TEZ/IVA on the intestinal microbiome of children with CF. We therefore undertook a longitudinal study to identify changes in clinical outcomes and the intestinal microbiomes of pediatric patients following the initiation of ELX/TEZ/IVA. To our knowledge, this study represents the first comprehensive study of the highly effective CFTR modulator formulation ELX/TEZ/IVA on the intestinal microbiome of children with CF.

2. METHODS

2.1 Recruitment of Subjects

Pediatric patients with a diagnosis of CF at Monroe Carell Jr. Children's Hospital at Vanderbilt (MCJCHV) were recruited beginning in July 2017 with follow-up until October 2022. Patients with the Phe508 CFTR mutation who were deemed eligible for ELX/TEZ/IVA by their pulmonologist were eligible for this study. Patients previously treated with other CFTR modulator regimens were permitted. Patients with pre-existing non-CF gastrointestinal disease were excluded. A total of 39 participants were recruited (Table 1). Informed consent was obtained from parental guardians, and assent was obtained from pediatric subjects in accordance with institutional research ethics guidelines. This study was approved by the MCJCHV Institutional Review Board (IRB # 200396). The lead investigators of this study had no direct role in the patients' routine medical care. All study data were stored in a Research Electronic Data Capture (REDCap) database per institutional guidelines (32).

2.2 Study Timepoints

Our analysis included stool samples from up to four timepoints per patient: two timepoints before ELX treatment (T1 & T2) and two timepoints after initiating ELX/TEZ/IVA (T3 & T4) (Fig. 1B). For clinical outcomes, data was either analyzed by individual timepoints (T1-T4) or time points were combined for pre-ELX/TEZ/IVA samples (T1 & T2 combined) and post-ELX-TEZ/IVA samples (T3 & T4 combined). Analysis of individual timepoints permitted assessment of additional differences between the 6 to 12-month periods after ELX/TEZ/IVA initiation. For microbiome comparisons, analysis was based on combined pre-ELX/TEZ/IVA samples (T1 & T2) and post-ELX-TEZ/IVA samples (T3 & T4).

2.3 Stool Sample Collection and DNA Extraction

Stool samples were collected prior to ELX/TEZ/IVA initiation, either through targeted collection as part of this study or from our center's biobank of CF stool samples (33, 34). Subsequent stool

samples were collected at approximately 6- and 12-month intervals after initiation of ELX/TEZ/IVA (Fig. 1A). Fecal samples were collected in sterile collection cups and refrigerated until transport to the laboratory. Patients who were unable to provide a stool sample in clinic were provided with an OMNIgene®•GUT stool collection kit for at home collection and stabilization, returned via overnight shipping, and stored according to manufacturer specifications. Aliquots of stool samples were aseptically aliquoted into cryovials in a laminar flow biosafety cabinet to minimize aerosols and stored at -80ºC until processing. Percent predicted forced expiratory volume in one second ($ppFEV_1$) values were obtained in the outpatient setting at the time of stool sample collection; the highest spirometry value of three attempts was recorded. Clinical data including body mass index (BMI, percentiles), percentage predicted forced expiratory volume in 1 second ($ppFEV_1$), medications, and laboratory values were recorded for visits when a stool sample was collected. Total DNA was extracted from 114 stool samples using QIAamp PowerFecal Pro DNA Kits according to the manufacturer's instructions. Bead beating for efficient lysis was conducted for 10 minutes. All steps, excluding bead beating and centrifugation, were conducted in a laminar flow biosafety cabinet. No human DNA depletion or enrichment of microbial DNA was performed. DNA yield was estimated by spectrophotometry (NanoDrop™2000c) in parallel with ensuring satisfactory A260/A280 ratio for DNA purity.

2.4 Fecal Calprotectin Measurements

Fecal calprotectin was measured using the Calprotectin ELISA Assay Kit (Eagle Biosciences). Duplicate portions of stool (50-100mg) were weighed and processed according to the manufacturer's instructions. Absorbance was measured with a SpectraMax® i3x (Molecular Devices). Fecal calprotectin (µg/g feces) was calculated using a 7-point standard curve. The assay's reported normal cut-off is <43.2 µg/g.

2.5 Shotgun Metagenomic Sequencing

Sequencing libraries were prepared using Illumina® reagents as described elsewhere (35). Pooled libraries were sequenced on NextSeq2000 to generate 150-bp paired-end reads. An average of 13.9 million reads were produced per sample (range 9.1 to 30.1 million). Sequencing adaptors and low-quality sequences were trimmed with fastq-mcf from ea-utils-1.1.2.779 using default parameters (Supplementary Methods) (36).

2.6 Taxonomic and Functional Profiling of Metagenomic Sequence Data

Species abundances were determined with MetaPhlAn4 following read alignment to the MetaPhlan4 database (37). Diversity metrics were calculated with the vegan R package (38) and plotted with ggplot2. A weighted UniFrac distance matrix was constructed with the MetaPhlAn R script "calculate_unifrac". Functional profiling was conducted with HUMAnN 3.0 with mapping to UniRef90 gene-families and MetaCyc metabolic pathways (39–41). UniRef90 gene-families were reformatted into KEGG orthology (KO) groups using the HUMAnN command "humann_regroup_table". In total, we identified 722 species, 526 MetaCyc pathways, and 8634 distinct KO groups annotations in the 114 samples. All functional annotations were normalized using the HUMAnN command "humann_renorm_table --units cpm". Antibiotic resistance genes were identified by ShortBRED (42) with the reference Comprehensive Antibiotic Resistance Database (CARD version 2017) (43). ARG abundance was calculated as reads per kilobase of reference sequence per million sample reads (RPKM).

2.7 Microbial Dysbiosis Index

The Microbial Dysbiosis Index (MD-index) was calculated as the log10 of the ratio of the relative abundance of taxa which were previously positively and negatively associated with newly diagnosed pediatric Crohn's disease (44). Specifically, the numerator includes *Enterobacteriaceae*, *Pasteurellaceae*, *Fusobacteriaceae*, *Neisseriaceae*, *Veillonellaceae*, *Gemellaceae*; the denominator includes *Bacteroidales*, *Clostridiales* (excluding *Veillonellaceae*), *Erysipelotrichaceae*, and *Bifidobacteriaceae*. Higher indices correspond to a greater inflammatory taxonomic profile. The MD-index has been previously applied to stool samples of children with CF (14, 45).

2.8 Differential Abundance Testing

We used MaAsLin2 (Microbiome Multivariable Associations with Linear Models, Maaslin2 R package) to identify differentially abundant features (46). We included ELX/TEZ/IVA, age, and recent antibiotic exposure as fixed effects. Subject ID was specified as a random effect due to multiple samples from the same subject. Species, KEGG orthologs, and MetaCyc pathways detected at least 10% of samples were tested (i.e., prevalence = 0.1); no minimum abundance was specified. Abundances were log transformed within the MaAsLin2 function. The general linear "LM" model was used. MaAsLin2 coefficients are equivalent to log2(FoldChange). The Benjamini-Hochberg procedure was used to correct P values, and corrected P values are reported as False Discovery Rates (FDR).

2.9 Statistical Analyses

Statistical analyses were conducted using GraphPad Prism 9 and R (version 4.2.1) software. Details of the statistical tests used and the significance thresholds are presented in the figure legends. All box-plot graphs are defined as: center line—median; box limits—upper and lower quartiles; whiskers—1.5× interquartile range.

2.10 Reproducibility and Data Availability

The results can be reproduced using raw sequence data that are available on NCBI-Genbank databases under BioProject PRJNA948536 or using processed data in the Supplementary Dataset 1. Bioinformatic code is available within the repository https://github.com/reaset41/CF-GI-Microbiome-ELX-TEZ-IVA.

3. RESULTS

3.1 Study Cohort and Stool Sample Collection

Stool samples were collected from a total of 39 children with CF (Table 1). The median (IQR) age of participants at the time of ELX/TEZ/IVA initiation was 9.86 years old (8.87, 12.15) and 53.4% were male. Of these, 35.9% (14/39 subjects) had CFTR modulator use (at any time) before ELX/TEZ/IVA. Patients provided an average of 2.92 stool samples with all patients providing at least one stool sample prior to starting ELX/TEZ/IVA (T1 median= 33.6 months before ELX/TEZ/IVA initiation, IQR 28.6, 36.7 months and T2 median=0.64 months before ELX/TEZ/IVA initiation, IQR 0.13, 2.2 months). Subsequent stool samples were collected at approximately 6- and 12-month intervals (T3 median=5.97 months, IQR 5.38, 6.92 months and T4 median=12.39 months, IQR 11.1, 13.1 months). There was a total of 114 stool samples with 53 samples before ELX/TEZ/IVA therapy and 61 samples after ELX/TEZ/IVA treatment (Fig. 1A & S2). Of the 53 samples collected pre-ELX/TEZ/IVA, 8 samples (15%) were collected while the patient was receiving an alternative CFTR modulator (Supplementary Dataset 1).

3.2 Clinical Improvement after ELX/TEZ/IVA

To determine our cohort's clinical response to ELX/TEZ/IVA, we compared clinical metrics from before and after ELX/TEZ/IVA initiation. Both BMI percentile and $ppFEV_1$ increased in the timepoints after ELX/TEZ/IVA compared to pre-ELX/TEZ/IVA timepoints (Fig. 1C-D & S1A-B). Median BMI percentile increased from the 54^{th} percentile to the 67^{th} percentile after ELX/TEZ/IVA (Fig. 1D). Likewise, there was a mean change in $ppFEV_1$ of 12.3 percentage points (95% CI 6.7-17.8) before and after ELX/TEZ/IVA (Fig. 1C). Between 6- and 12-months

after ELX/TEZ/IVA, there was no further significant improvement in either BMI or ppFEV$_1$ (Fig. S1A-B, T3 & T4). Consistent with increased BMI, weight percentile increased after ELX/TEZ/IVA (Fig. S1C). Height percentile increased between T2 and both T3 and T4 (Fig. S1D, P=0.013, P=0.026, respectively), though not between T1 and T3 & T4. Total antibiotic days per patient were aggregated and decreased from a median of 22.5 days per 6-months before ELX/TEZ/IVA to 0 antibiotic days per 6-months after ELX/TEZ/IVA (Fig. 1E, P<0.0001).

3.3 Microbiome Diversity Increases After ELX/TEZ/IVA

From shotgun metagenomic sequencing on 114 stool samples, we compared measures of microbiome taxonomy and diversity. In contrast to previously published CF microbiome datasets of infants (8, 22), our dataset of older children was dominated by the phylum Firmicutes with minimal Proteobacteria (Fig. 2A and Supplementary Dataset 1). Alpha diversity, as measured by the Shannon index and richness (observed species), significantly increased following ELX/TEZ/IVA (Fig. 2B-C, P=0.021 and P=0.026, respectively). The number of species observed increased from a median (IQR) of 83 (62, 115) species before ELX/TEZ/IVA to 109 (82,125) species after ELX/TEZ/IVA (Fig. 2B). The cumulative increases in alpha diversity were not significantly different when comparing between the four timepoints individually (Fig. S2A-B), and there were no differences in overall community composition (beta-diversity) before and after ELX/TEZ/IVA (Fig. S2C-D).

To determine the effect of prior CFTR modulator treatment besides ELX/TEZ/IVA, we compared diversity metrics between modulator naïve samples (samples=45) and samples collected while subjects were receiving another CFTR modulator (samples=8) before ELX/TEZ/IVA. Samples collected while subjects were receiving another CFTR modulator had similar diversity to modulator naïve samples (Fig. S3A-B). Following ELX/TEZ/IVA, samples from subjects who had previously received another modulator (samples=20) had similar improvements in microbiome diversity to samples from subjects who had not previously received another modulator (samples=41), indicating that the residual effects of another modulator did not influence microbiome diversity improvement on ELX/TEZ/IVA (Fig. S3C-D).

To determine the influence of antibiotic exposure on microbiome diversity measures regardless of ELX/TEZ/IVA status, we categorized patient stool samples as having received antibiotics within the six-months prior to stool sample collection (samples=62) or no antibiotic receipt (samples=52). Recent antibiotic exposure significantly impacted alpha diversity measures reducing Shannon diversity and richness (Fig. 2D-E). Likewise, population structure

(beta-diversity) was significantly different between samples with and without recent antibiotic exposure (Fig. S2E, permutational multivariate analysis of variance [PERMANOVA]=0.003).

3.4 Microbiome Encoded Antibiotic Resistance Genes Decrease After ELX/TEZ/IVA

As discussed above, patients required far fewer antibiotics after starting ELX/TEZ/IVA (Fig. 1E & S4A). Since the intestinal microbiome is a reservoir of antibiotic resistant genes (ARGs) (47), we compared the number and type of intestinal ARGs before and after ELX/TEZ/IVA initiation. Across the 114 samples, we detected a total of 309 unique ARGs. The median number of unique ARGs nominally decreased from a median 86 ARGs (IQR 40, 96) before ELX/TEZ/IVA to a median 68 ARGs (IQR 38, 90) after ELX/TEZ/IVA (Fig. S4B, P=0.31). ARG abundance decreased from a median of 1180 RPKM (IQR 815.4, 1761.1) to 829 RPKM (IQR 460.5, 1299.0) (Fig. 3A, P=0.0097) though this effect was likely mediated by reduced antibiotic use.

Next, we aggregated the relative abundance of ARGs by antibiotic class to which they confer resistance (Fig. 3B). The abundance of ARGs conferring resistance to peptide antibiotics and ungrouped antibiotics (“Other”) significantly decreased after ELX/TEZ/IVA (Fig. 3B & S4C-E, P=0.012, P=0.022 respectively). The most prevalent antibiotics within the peptide ARG class included *arnA* (samples=72/114), *yojI* (samples=71/114), *pmrF* (samples=74/114) and *pmrC* (samples=71/114). *arnA, pmrF* and *pmrC* modify Lipid A on bacterial cells to repel cationic peptide antibiotics, whereas *yojI* is a peptide efflux pump. The most prevalent ARGs within the “Other” group were *fabI* (samples=84/114), *gadE* (samples=78/114), and EF-Tu mutations (samples=75/114). These ARGs or mutations confer resistance to isoniazid/disinfecting agents (*fabI*), acid resistance and efflux pump (*gadE*), and elfamycin (EF-Tu). Despite being the most prevalent, none of these ARGs were independently altered in abundance following ELX/TEZ/IVA (Fig. S4D & S4F).

3.5 Alterations to Specific Bacterial Taxa Following ELX/TEZ/IVA

To determine whether specific bacterial taxa change following ELX/TEZ/IVA treatment, we used MaAsLin2 (Microbiome Multivariable Associations with Linear Models) to identify differentially abundant microbial taxa (46). No phyla were differentially abundant following ELX/TEZ/IVA (Fig. 2A & Table S4). At a granular taxonomic level, seventeen species were differentially abundant between samples before and after ELX/TEZ/IVA (FDR<0.1, Fig. 4A and Table S3), with eleven species increasing in abundance after ELX/TEZ/IVA, and six species decreasing. The three species with the lowest FDR and, therefore, highest reliability were

Butyricicoccus SGB14985, *S. aureus,* and *Roseburia faecis* (Fig. 4A-B). *Butyricicoccus* SGB14985, an uncultivated species, was decreased in abundance following ELX/TEZ/IVA (fold change 0.16, FDR=0.022). *Roseburia faecis* was increased in abundance following ELX/TEZ/IVA (fold change 7.35, FDR=0.025) and negatively correlated with recent antibiotic exposure (Fig. S5A, fold change 0.20, FDR=0.086). The intestinal tract has immunological cross-talk between the separate but similarly structured mucosal environment of the lung, deemed the gut-lung axis (20). Since the intestinal tract can harbor similar respiratory pathogens in patients with CF (15, 48, 49), we performed focused analysis of CF pathogens. *S. aureus*, the predominant respiratory pathogen in children with CF (50), was decreased in abundance after ELX/TEZ/IVA (Fig. 4A-B, fold change 0.40, FDR=0.042). Other members of the respiratory microbiota which are frequently detected in the intestines (14, 15)—specifically the genera *Haemophilus*, *Prevotella*, *Streptococcus*, *Veillonella*—did not significantly change after ELX/TEZ/IVA initiation (Fig. S5B). *Pseudomonas aeruginosa*, an additional respiratory pathogen of importance in CF, was detected in only two of the 114 stool samples. Furthermore, fungal taxa were only identified in 8/114 samples (Supplementary Dataset 1).

3.6 Intestinal Inflammation Decreases After ELX/TEZ/IVA

Fecal calprotectin was measured across the four timepoints and markedly decreased following ELX/TEZ/IVA (Fig. 5A & S5A). Overall, mean fecal calprotectin decreased from 109 µg/g before ELX/TEZ/IVA to 44.8 µg/g for a mean decrease of 64.2 µg/g (95% CI -16.1, -112.3, Fig. 5A). We then computed the microbial dysbiosis index (MD-index), a ratio of bacterial taxa positively and negatively associated with newly diagnosed pediatric Crohn's disease, to assess the relationship between intestinal inflammation and specific microbial signatures (44). We noted a nominal reduction in the MD-index following ELX/TEZ/IVA (Fig. 5B, P=0.068), which was less pronounced when comparing samples from patients with recent antibiotic exposure and those without (Fig. 5C, P=0.77).

3.7 Microbiome Functional Changes Reveal Specific Disease-Relevant Changes

From the 114 stool samples, alignment of sequencing reads to known microbial proteins and pathways identified 8634 KEGG orthology (KO) protein groups and 526 MetaCyc metabolic pathways, consistent with prior studies of the intestinal microbiota (51). There were 249 KO groups differentially abundant with respect to ELX/TEZ/IVA use (MaAsLin2 FDR<0.25, Fig. 5D & Table S6). Strikingly, a common thread among differentially abundant KO groups was a decreased abundance of genes encoding oxidative phosphorylation functions following

ELX/TEZ/IVA (Fig. 5D). Seven of the top 10 most differentially abundant KO groups were components of the electron transport chain (Fig. 5D & S5B and Table S7) and included NADH-ubiquinone oxidoreductases (e.g., K03883, K03881, K03884, & K03880), F-type ATPase subunits (e.g., K02125), and cytochrome c oxidase subunits (e.g., K02262, K02261, & K02256). The taxa contributing to oxidative phosphorylation KO groups were not consistently annotated by HUMAnN (Fig. S6C and Table S10). This indicates that a specific taxonomic signature was not responsible for the reduced abundance of oxidative phosphorylation KO groups (Fig. S6C). These results were corroborated by MaAsLin2 differential abundance testing of MetaCyc pathways. Sixty-four MetaCyc pathways were differentially abundant with respect to ELX/TEZ/IVA use (MaAsLin2 FDR<0.25, Fig. 5E & S7, Table S9). Two of these pathways corresponded to aerobic respiration (PWY-3781 and PWY-7279). Differential abundance of anaerobic energy metabolism pathways showed discordant results with one pathway increased in abundance following ELX/TEZ/IVA (PWY-7383), and two pathways decreased in abundance (PWY-7389 and PWY-7384) following ELX/TEZ/IVA (Fig. S7 and Table S9). Thirteen amino acid biosynthesis pathways were universally prevalent in all stool samples (114/114) and significantly increased in abundance following ELX/TEZ/IVA (Fig. 5E and Table S9, FDR<0.25). This indicates increased biosynthetic capacity of the intestinal microbiome following ELX/TEZ/IVA.

Furthermore, multiple pathways related to nucleobase and nucleotide metabolism were differentially abundant following ELX/TEZ/IVA. Pyrimidine deoxyribonucleotide biosynthesis pathways were reduced in abundance following ELX/TEZ/IVA (PWY-7184 & PWY-6545) whereas a pyrimidine ribonucleotides biosynthesis pathway was increased in abundance (PWY0-162, Fig.S7 and Table S9). While these general pyrimidine deoxyribonucleotide biosynthesis pathways were reduced in abundance, specific pathways for thiamine biosynthesis (PWY-7357) and two uridine-monophosphate biosynthesis pathways (PWY-7790 & PWY−7791) were significantly increased in abundance following ELX/TEZ/IVA. An anaerobic pathway for purine degradation was increased in abundance following ELX/TEZ/IVA (P164-PWY). Three pathways related to allantoin degradation were significantly reduced in abundance following ELX/TEZ/IVA (PWY-5692, PWY0-41 & URDEGR-PWY, Fig. S7 and Table S9).

Another intriguing observation was the reduced abundance of KO groups involved in acid tolerance and transport following ELX/TEZ/IVA (Fig. 5D). KO groups involved in organic acid transport (e.g., K03290 & K23016) and proton-symporters (e.g., K11102 & K03459) were reduced in abundance following ELX/TEZ/IVA. Likewise, an acidity-responsive transcriptional

regulator (K03765, *cadC*) was decreased in abundance following ELX/TEZ/IVA (Fig. 5D and Table S7, fold change 0.42, FDR=0.27).

4. DISCUSSION

ELX/TEZ/IVA has changed the trajectory of CF patient care and dramatically improved clinical outcomes. Nutritional status and components of the intestinal microbiome are strong predictors of future clinical outcomes, particularly in children with CF (6–8). We therefore sought to determine the effects of ELX/TEZ/IVA on intestinal inflammation and the intestinal microbiome in children with CF. Herein, we present a comprehensive longitudinal characterization of the intestinal microbiome in children with CF treated with ELX/TEZ/IVA. We identified widespread changes to the intestinal microbiome after ELX/TEZ/IVA including taxonomic composition, reduced carriage of ARGs, and altered microbiota metabolic functions.

Although randomized controlled trials demonstrated that ELX/TEZ/IVA was safe and effective, there are limited post-approval clinical data, particularly in children over two years old (52–56). BMI and $ppFEV_1$ are useful markers of clinical response to CFTR modulator treatment in children (57). Our cohort demonstrated significant improvement in $ppFEV_1$ and BMI percentile within six-months of starting ELX/TEZ/IVA, with no additional differences at later time points (Fig. S1A-B). This is consistent with prior clinical trial and real-world data showing the greatest impact on nutritional status and anthropometric parameters immediately after ELX/TEX/IVA therapy initiation with subsequent plateau without regression in children (52, 56, 58). Prior baseline BMI, particularly underweight status, has been predicted to be a major determinant of increase in weight gain in patients with CF treated with ELX/TEZ/IVA (59). Furthermore, between the timepoint immediately before ELX/TEZ/IVA initiation (T2) and post-ELX/TEZ/IVA timepoints (T3 & T4), there was a significant increase in height percentile (Fig. S1D). This suggests that CFTR modulator therapy may improve linear growth in children with CF. In sum, these results support the clinical responsiveness of children with CF to ELX/TEZ/IVA.

The gastrointestinal microbiome influences whole-body physiology. CF intestinal microbiome abnormalities begin in infancy, diverging from healthy controls soon after birth (8, 14, 15, 21–23). Intriguingly, the microbiome of patients with CF resembles that of patients with IBD, a group with a characteristically perturbed intestinal microbiome (12, 45, 60). Considerable prior research has characterized the development of the CF intestinal microbiome in infants (8, 13–15, 21–23). Less information exists about the CF intestinal microbiome in children and adolescents (13, 24, 26, 61–65). A consistent finding is that high levels of the phylum Proteobacteria, specifically the species *Escherichia coli*, define the infant CF intestinal

microbiome (12, 22). The abundance of Proteobacteria decreases with age in young children with CF (14, 22). In our dataset of older children with CF, Proteobacteria comprised a minority of the identified bacteria (Fig. 2A). In turn, the relative abundance of the phylum Firmicutes is increased in our cohort, likely representing a more stable “adult-like” microbiome.

Direct comparison of our results to studies containing healthy controls is difficult given different sampling and sequencing methodologies. Notably, although our study identified subtle changes in the intestinal microbiome after initiation of ELX/TEZ/IVA in children with CF, the post-ELX/TEZ/IVA intestinal microbiome remains significantly altered from what has been described in healthy children. Compared to healthy children, the intestinal microbiome of children with CF is delayed in development and exhibits decreased microbial diversity relative to healthy controls throughout childhood and adolescence (22, 24, 63). Among the most consistent differences between healthy controls and patients with CF is reduced abundance of the phylum Bacteroidetes in patients with CF (13, 20, 61, 63, 66). In our dataset, Bacteroidetes remained depleted post-ELX/TEZ/IVA (Fig. 2A and Table S4). Likewise, Shannon diversity remained below that of similarly-aged healthy controls (24, 63), as discussed henceforth.

In our cohort, alpha diversity, as measured by the Shannon index and richness (observed species), significantly increased following ELX/TEZ/IVA (Fig. 2B-C). These results demonstrate modest but statistically significant differences in an older cohort of children with CF, whose microbiome resembles that of more of a stable “adult-like” microbiome. The difference in the median Shannon diversity was increased 0.29 after ELX/TEZ/IVA (Fig. 2B). In contrast, a similarly aged cohort of children with CF exhibited a median ~1.0 reduced Shannon index compared to healthy controls in the same study (24). Thus, while our cohort exhibited significant increases in Shannon diversity, it is unlikely that this magnitude of increase restores the diversity to that of similarly aged healthy controls. This is consistent with the notion that “adult-like” intestinal microbiota are remarkably stable and resilient to intervention (67–69). As CFTR modulator formulations are approved for younger children, particularly infants for whom the microbiome is still developing, studying the effects of CFTR modulators on the developing intestinal microbiome will be an important research endeavor and may show more substantial differences.

In children with CF, markers of intestinal inflammation correlate with growth failure (11, 24). Moreover, intestinal inflammation in patients with CF is linked to higher rates of IBD and colorectal cancer in patients with CF (16, 17, 70). Fecal calprotectin, a laboratory marker of intestinal inflammation (71–73), significantly decreased following ELX/TEZ/IVA (Fig. 5A), corroborating prior reports in the PROMISE and RECOVER cohorts (74, 75). Using a dysbiosis

index of bacterial taxa correlated with pediatric Crohn's disease (44), we identified that this dysbiosis index nominally decreased following ELX/TEZ/IVA initiation (Fig. 5B). The decrease in the median MD-index was 0.166 before and after ELX/TEZ/IVA. The median post-ELX/TEZ/IVA MD-index was lower (i.e. reduced inflammatory taxa) than that of healthy controls in the original publication describing the MD-index (44). This suggests that the magnitude of decrease in the MD-index in our study may be biologically meaningful. Furthermore, the difference between pre- and post-ELX/TEZ/IVA (Fig. 5B) was more pronounced than in samples with and without recent antibiotic exposure (Fig. 5C). This suggests that this effect may be specific to ELX/TEZ/IVA treatment, and not due to reduced antibiotic use. At the species level, the butyrate-producing species *Roseburia faecis* was significantly enriched following ELX/TEZ/IVA (Fig. 4A-B). Prior studies have identified *R. faecis* as reduced in abundance in patients with CF (20, 76–78). In parallel, we detected reduced abundance of genes involved in oxygen-dependent metabolism following ELX/TEZ/IVA (Fig. 5D-E). Intestinal inflammation is characterized by a shift towards oxygen-dependent microbiota metabolism, perpetuating a cycle of inflammatory damage (79–81). From multiple lines of evidence, our results suggest that ELX/TEZ/IVA reduces intestinal inflammation in children with CF.

Respiratory infections require frequent antibiotics in patients with CF. Some respiratory pathogens also colonize the intestinal tract and temporally correlate with respiratory colonization (15, 48, 49). *S. aureus* is among the first pathogens to colonize the respiratory tract and cause infections in children with CF (50). We detected reduced intestinal abundance of *S. aureus* following ELX/TEZ/IVA (Fig. 4A-B). Antibiotic exposure in patients with CF has been associated with increased intestinal carriage of antibiotic resistant bacteria compared to healthy controls which are a poor prognostic factor (82–84). Following ELX/TEZ/IVA, patients in our cohort required far fewer antibiotics (Fig. 1E). In turn, we detected reduced intestinal abundance of ARGs (Fig. 2E). These results indicate disease-relevant taxonomic changes to the intestinal microbiome following ELX/TEZ/IVA, as well as reduced ARGs.

The CFTR channel permits transepithelial movement of bicarbonate ($HCO3^-$) and chloride (Cl^-) (5). Intestinal pH is lower in patients with CF due to the lack of neutralizing bicarbonate (85) yet increases with CFTR modulator treatment, consistent with increased CFTR activity in the intestinal tract (86). We observed a reduced abundance of microbial protein groups associated with acid tolerance (Fig. 5D), consistent with microbial adaptation to increased CFTR channel function in the intestines. These results display physiologically intuitive functional changes to the microbiome post-ELX/TEZ/IVA. As CFTR modulators become the

mainstay of treatment for CF, further research will be necessary to mechanistically describe the effects of CFTR modulators on gastrointestinal function.

Our study is strengthened by longitudinal sampling over a five-year period combined with the real-world use of ELX/TEZ/IVA. Using shotgun metagenomic sequencing, we comprehensively compared microbiota differences before and after ELX/TEZ/IVA. Sampling of the intestinal microbiome over extended periods will be important to uncover additional long-term improvements to the microbiome. Similarly, further research is necessary to delineate the effects of ELX/TEX/IVA on the interconnected respiratory and intestinal microbiomes. Although our study was limited by the single-center focus, our cohort mirrors the overall CF pediatric population in clinical and demographic factors (Table 1). Our study lacks untreated CF controls or healthy controls, which would allow for additional comparisons.

In summary, our results indicate that the CFTR modulator ELX/TEZ/IVA alters the intestinal microbiome in children with CF. We identified taxonomic and functional changes to the intestinal microbiome that represent improvements to CF intestinal microbiome structure and function. Our results also support that CFTR modulators reduce intestinal inflammation in children with CF.

AUTHOR CONTRIBUTIONS (CRediT author statement)

SAR: Investigation, Methodology, Data Curation, Formal analysis, Writing - Original Draft

RB: Conceptualization, Funding Acquisition, Investigation, Data Curation, Writing - Original Draft

AW: Investigation, Software

KP: Investigation

JS: Investigation

AGS: Supervision, Writing - Review & Editing

RFB: Supervision, Writing - Review & Editing

KME: Supervision, Writing - Review & Editing

SJS: Investigation, Data Curation, Software, Writing - Review & Editing

MH: Supervision, Writing - Review & Editing

MRN: Conceptualization, Funding Acquisition, Investigation, Supervision, Writing - Original Draft

ACKNOWLEDGEMENTS AND FUNDING

We would like to express our sincere appreciation to the patients and their families who enthusiastically participated in this study. We would like to thank our advanced practitioner and nursing colleagues from the Pediatric Pulmonology clinic at the Monroe Carrell Jr. Children's

Hospital at Vanderbilt for their collegiality and assistance with this study. This work was supported, in part, by National Institutes of Health (NIH) grants T32DK007673 (RB), K23AI156132 (MRN), F30AI169748 (SAR), T32GM007347 (SAR), and P30DK089507 (SJS); the Cystic Fibrosis Foundation (SINGH19R0 to SJS) and the Thrasher Research Fund (RB and MRN).

CONFLICTS OF INTERESTS

All authors declare that they have no conflicts of interest relevant to this work.

DATA AVAILABILITY

All sequence data derived from this work are publicly available in NCBI-Genbank databases under BioProject PRJNA948536. All processed data and code used for bioinformatic analysis is available within the repository: https://github.com/reaset41/CF-GI-Microbiome-ELX-TEZ-IVA.

AUTHOR ORCID IDs:

SAR: 0000-0002-7791-1641
RB: 0000-0002-6689-5658
AW: 0000-0002-5202-1108
KP: 0000-0003-1454-6381
AGS: 0000-0002-5495-1237
RFB: 0000-0003-3632-4587
KME: 0000-0003-3912-9832
SJS: 0000-0001-8355-6992
MH: 0000-0003-4249-8997
MRN: 0000-0003-3941-5599

REFERENCES

1. 2022. CF Foundation Estimates Increase in CF Population. Cystic Fibrosis Foundation. https://www.cff.org/news/2022-07/cf-foundation-estimates-increase-cf-population. Retrieved 10 April 2023.
2. Moshiree B, Freeman AJ, Vu PT, Khan U, Ufret-Vincenty C, Heltshe SL, Goss CH, Schwarzenberg SJ, Freedman SD, Borowitz D, Sathe M. 2022. Multicenter prospective study showing a high gastrointestinal symptom burden in cystic fibrosis. Journal of Cystic Fibrosis https://doi.org/10.1016/j.jcf.2022.10.006.
3. De Lisle RC, Borowitz D. 2013. The cystic fibrosis intestine. Cold Spring Harb Perspect Med 3:1–18.
4. Kreda SM, Davis CW, Rose MC. 2012. CFTR, mucins, and mucus obstruction in cystic fibrosis. Cold Spring Harb Perspect Med 2.
5. Elborn JS. 2016. Cystic fibrosis. The Lancet 388:2519–2531.

6. Steinkamp G, Wiedemann B. 2002. Relationship between nutritional status and lung function in cystic fibrosis: Cross sectional and longitudinal analyses from the German CF quality assurance (CFQA) project. Thorax 57:596–601.
7. Ashkenazi M, Nathan N, Sarouk I, Aluma BEB, Dagan A, Bezalel Y, Keler S, Vilozni D, Efrati O. 2019. Nutritional Status in Childhood as a Prognostic Factor in Patients with Cystic Fibrosis. Lung https://doi.org/10.1007/s00408-019-00218-3.
8. Hayden HS, Eng A, Pope CE, Brittnacher MJ, Vo AT, Weiss EJ, Hager KR, Martin BD, Leung DH, Heltshe SL, Borenstein E, Miller SI, Hoffman LR. 2020. Fecal dysbiosis in infants with cystic fibrosis is associated with early linear growth failure. Nat Med 26:215–221.
9. Rogers GB, Carroll MP, Hoffman LR, Walker AW, Fine DA, Bruce KD. 2010. Comparing the microbiota of the cystic fibrosis lung and human gut. Gut Microbes 1:85–93.
10. Héry-arnaud G, Boutin S, Cuthbertson L, Elborn SJ, Tunney MM. 2019. The lung and gut microbiome: what has to be taken into consideration for cystic fibrosis ? Journal of Cystic Fibrosis 18:13–21.
11. Dhaliwal J, Leach S, Katz T, Nahidi L, Pang T, Lee JM, Strachan R, Day AS, Jaffe A, Ooi CY. 2015. Intestinal inflammation and impact on growth in children with cystic fibrosis. J Pediatr Gastroenterol Nutr 60:521–526.
12. Hoffman LR, Pope CE, Hayden HS, Heltshe S, Levy R, McNamara S, Jacobs MA, Rohmer L, Radey M, Ramsey BW, Brittnacher MJ, Borenstein E, Miller SI. 2014. Escherichia coli dysbiosis correlates with gastrointestinal dysfunction in children with cystic fibrosis. Clinical Infectious Diseases 58:396–399.
13. Manor O, Levy R, Pope CE, Hayden HS, Brittnacher MJ, Carr R, Radey MC, Hager KR, Heltshe SL, Ramsey BW, Miller SI, Hoffman LR, Borenstein E. 2016. Metagenomic evidence for taxonomic dysbiosis and functional imbalance in the gastrointestinal tracts of children with cystic fibrosis. Sci Rep 6:1–9.
14. Price CE, Hampton TH, Valls RA, Barrack KE, O'Toole GA, Madan JC, Coker MO. 2023. Development of the intestinal microbiome in cystic fibrosis in early life. mSphere https://doi.org/10.1128/msphere.00046-23.
15. Madan JC, Koestle DC, Stanton BA, Davidson L, Moulton LA, Housman ML, Moore JH, Guill MF, Morrison HG, Sogin ML, Hampton TH, Karagas MR, Palumbo PE, Foster JA, Hibberd PL, O'Toole GA. 2012. Serial analysis of the gut and respiratory microbiome in cystic fibrosis in infancy: Interaction between intestinal and respiratory tracts and impact of nutritional exposures. mBio 3.
16. Hadjiliadis D, Khoruts A, Zauber AG, Hempstead SE, Maisonneuve P, Lowenfels AB, Braid AL, Cullina J, Daggett A, Fink A, Gini A, Harron PF, Lansdorp-Vogelaar I, Lieberman D, Liou T, Lomas P, Marshall B, Meyer K, Rustgi A, Shaukat A, Sabadosa K. 2018. Cystic Fibrosis Colorectal Cancer Screening Consensus Recommendations. Gastroenterology 154:736-745.e14.
17. Hegagi M, Aaron SD, James P, Goel R, Chatterjee A. 2017. Increased prevalence of colonic adenomas in patients with cystic fibrosis. Journal of Cystic Fibrosis 16:759–762.
18. Schwarzenberg SJ, Wielinski CL, Shamieh I, Carpenter BLM, Jessurun J, Weisdorf SA, Warwick WJ, Sharp HL. 1995. Cystic fibrosis-associated colitis and fibrosing colonopathy. J Pediatr 127:565–570.

19. Burton S, Hachem C, Abraham J. 2021. Luminal Gastrointestinal Manifestations of Cystic Fibrosis. Curr Gastroenterol Rep 23.
20. Price CE, O'Toole GA. 2021. The gut-lung axis in cystic Fibrosis. J Bacteriol. American Society for Microbiology https://doi.org/10.1128/JB.00311-21.
21. Antosca KM, Chernikova DA, Ruoff KL, Li K, Guill MF, MacKenzie TA, Dorman DB, Moulton LA, Williams MA, Aldrich BJ, Yuan IH, Karagas MR, O'Toole GA, Madan JC. 2019. Altered Stool Microbiota of Infants with Cystic Fibrosis Shows Reduction in Genera Associated with Immune Programming. J Bacteriol 201:1–15.
22. Salerno P, Verster AJ, Valls RA, Barrack KE, Price CE, Madan JC, O'Toole GA, Ross BD. 2023. Persistent delay in maturation of the developing gut microbiota in infants with cystic fibrosis. bioRxiv https://doi.org/10.1101/2023.05.02.539134.
23. Kristensen M, Prevaes SMPJ, Kalkman G, Tramper-Stranders GA, Hasrat R, de Winter-de Groot KM, Janssens HM, Tiddens HA, van Westreenen M, Sanders EAM, Arets B, Keijser B, van der Ent CK, Bogaert D. 2020. Development of the gut microbiota in early life: The impact of cystic fibrosis and antibiotic treatment. Journal of Cystic Fibrosis 19:553–561.
24. Coffey MJ, Nielsen S, Wemheuer B, Kaakoush NO, Garg M, Needham B, Pickford R, Ja A, Thomas T, Chee Y. Ooi. 2019. Gut Microbiota in Children With Cystic Fibrosis: A Taxonomic and Functional Dysbiosis. Sci Rep 9:1–14.
25. Hoen AG, Li J, Moulton LA, O'Toole GA, Housman ML, Koestler DC, Guill MF, Moore JH, Hibberd PL, Morrison HG, Sogin ML, Karagas MR, Madan JC. 2015. Associations between gut microbial colonization in early life and respiratory outcomes in cystic fibrosis. Journal of Pediatrics 167:138-147.e3.
26. Vernocchi P, Chierico F Del, Russo A, Majo F, Rossitto M, Valerio M, Casadei L, Storia A La, De Filippis F, Rizzo C, Manetti C, Paci P, Ercolini D, Marini F, Fiscarelli EV, Dallapiccola B, Lucidi V, Miccheli A, Putignani L. 2018. Gut microbiota signatures in cystic fibrosis: Loss of host CFTR function drives the microbiota enterophenotype. PLoS One 13:1–23.
27. Mahase E. 2019. Cystic fibrosis: Triple therapy shows promising results. The BMJ 367:6347.
28. Collins FS. 2019. Realizing the Dream of Molecularly Targeted Therapies for Cystic Fibrosis. New England Journal of Medicine 381:1862–1863.
29. Ooi CY, Syed SA, Rossi L, Garg M, Needham B, Avolio J, Young K, Surette MG, Gonska T. 2018. Impact of CFTR modulation with Ivacaftor on Gut Microbiota and Intestinal Inflammation. Sci Rep 8:1–8.
30. Ronan NJ, Einarsson GG, Deane J, Fouhy F, Rea M, Hill C, Shanahan F. 2022. Modulation , microbiota and inflammation in the adult CF gut□: A prospective study. Journal of Cystic Fibrosis https://doi.org/10.1016/j.jcf.2022.06.002.
31. Pope CE, Vo AT, Hayden HS, Weiss EJ, Durfey S, Mcnamara S, Ratjen A, Grogan B, Carter S, Nay L, Parsek M, Singh P, McKone E, Aitken M, Rosenfeld M, Hoffman L. 2020. Changes in fecal microbiota with CFTR modulator therapy: A pilot study. Journal of Cystic Fibrosis https://doi.org/10.1016/j.jcf.2020.12.002.
32. Harris PA, Taylor R, Thielke R, Payne J, Gonzalez N, Conde JG. 2009. Research electronic data capture (REDCap)-A metadata-driven methodology and workflow process for providing translational research informatics support. J Biomed Inform 42:377–381.

33. Reasoner SA, Fazili IF, Bernard R, Parnell JM, Sokolow AG, Thomsen KF, Edwards KM, Brown RF, Nicholson MR. 2022. Prevalence, Risk Factors, and Sequelae of Asymptomatic Clostridioides difficile Colonization in Children with Cystic Fibrosis. Journal of Cystic Fibrosis https://doi.org/10.1016/j.jcf.2022.12.014.
34. Parnell JM, Fazili I, Bloch SC, Lacy DB, Garcia-Lopez VA, Bernard R, Skaar EP, Edwards KM, Nicholson MR. 2021. Two-step Testing for Clostridioides Difficile is Inadequate in Differentiating Infection From Colonization in Children. J Pediatr Gastroenterol Nutr 72:378–383.
35. Gaio D, Anantanawat K, To J, Liu M, Monahan L, Darling AE. 2022. Hackflex: Low-cost, high-throughput, Illumina Nextera Flex library construction. Microb Genom 8.
36. Aronesty E. 2011. ea-utils: Command-line tools for processing biological sequencing data. https://github.com/ExpressionAnalysis/ea-utils.
37. Blanco-Míguez A, Beghini F, Cumbo F, McIver LJ, Thompson KN, Zolfo M, Manghi P, Dubois L, Huang KD, Thomas AM, Nickols WA, Piccinno G, Piperni E, Punčochář M, Valles-Colomer M, Tett A, Giordano F, Davies R, Wolf J, Berry SE, Spector TD, Franzosa EA, Pasolli E, Asnicar F, Huttenhower C, Segata N. 2023. Extending and improving metagenomic taxonomic profiling with uncharacterized species using MetaPhlAn 4. Nat Biotechnol https://doi.org/10.1038/s41587-023-01688-w.
38. Dixon P. 2003. VEGAN, A Package of R Functions for Community Ecology. Journal of Vegetation Science 14:927–930.
39. Franzosa EA, McIver LJ, Rahnavard G, Thompson LR, Schirmer M, Weingart G, Lipson KS, Knight R, Caporaso JG, Segata N, Huttenhower C. 2018. Species-level functional profiling of metagenomes and metatranscriptomes. Nat Methods 15:962–968.
40. Caspi R, Billington R, Keseler IM, Kothari A, Krummenacker M, Midford PE, Ong WK, Paley S, Subhraveti P, Karp PD. 2020. The MetaCyc database of metabolic pathways and enzymes-a 2019 update. Nucleic Acids Res 48:D455–D453.
41. Abubucker S, Segata N, Goll J, Schubert AM, Izard J, Cantarel BL, Rodriguez-Mueller B, Zucker J, Thiagarajan M, Henrissat B, White O, Kelley ST, Methé B, Schloss PD, Gevers D, Mitreva M, Huttenhower C. 2012. Metabolic reconstruction for metagenomic data and its application to the human microbiome. PLoS Comput Biol 8.
42. Kaminski J, Gibson MK, Franzosa EA, Segata N, Dantas G, Huttenhower C. 2015. High-Specificity Targeted Functional Profiling in Microbial Communities with ShortBRED. PLoS Comput Biol 11.
43. Jia B, Raphenya AR, Alcock B, Waglechner N, Guo P, Tsang KK, Lago BA, Dave BM, Pereira S, Sharma AN, Doshi S, Courtot M, Lo R, Williams LE, Frye JG, Elsayegh T, Sardar D, Westman EL, Pawlowski AC, Johnson TA, Brinkman FSL, Wright GD, McArthur AG. 2017. CARD 2017: Expansion and model-centric curation of the comprehensive antibiotic resistance database. Nucleic Acids Res 45:D566–D573.
44. Gevers D, Kugathasan S, Denson LA, Vázquez-Baeza Y, Van Treuren W, Ren B, Schwager E, Knights D, Song SJ, Yassour M, Morgan XC, Kostic AD, Luo C, González A, McDonald D, Haberman Y, Walters T, Baker S, Rosh J, Stephens M, Heyman M, Markowitz J, Baldassano R, Griffiths A, Sylvester F, Mack D, Kim S, Crandall W, Hyams J, Huttenhower C, Knight R, Xavier RJ. 2014. The treatment-naive microbiome in new-onset Crohn's disease. Cell Host Microbe 15:382–392.
45. Enaud R, Hooks KB, Barre A, Barnetche T, Hubert C, Massot M, Bazin T, Clouzeau H, Bui S, Fayon M, Berger P, Lehours P, Bébéar C, Nikolski M, Lamireau T, Delhaes L,

Schaeverbeke T. 2019. Intestinal Inflammation in Children with Cystic Fibrosis Is Associated with Crohn's-Like Microbiota Disturbances. J Clin Med 8:645.

46. Mallick H, Rahnavard A, McIver LJ, Ma S, Zhang Y, Nguyen LH, Tickle TL, Weingart G, Ren B, Schwager EH, Chatterjee S, Thompson KN, Wilkinson JE, Subramanian A, Lu Y, Waldron L, Paulson JN, Franzosa EA, Bravo HC, Huttenhower C. 2021. Multivariable association discovery in population-scale meta-omics studies. PLoS Comput Biol 17.

47. Salyers AA, Gupta A, Wang Y. 2004. Human intestinal bacteria as reservoirs for antibiotic resistance genes. Trends Microbiol https://doi.org/10.1016/j.tim.2004.07.004.

48. Wheatley RM, Caballero JD, van der Schalk TE, De Winter FHR, Shaw LP, Kapel N, Recanatini C, Timbermont L, Kluytmans J, Esser M, Lacoma A, Prat-Aymerich C, Oliver A, Kumar-Singh S, Malhotra-Kumar S, Craig MacLean R. 2022. Gut to lung translocation and antibiotic mediated selection shape the dynamics of Pseudomonas aeruginosa in an ICU patient. Nat Commun 13:6523.

49. Rogers GB, Carroll MP, Hoffman LR, Walker AW, Fine DA, Bruce KD. 2010. Comparing the microbiota of the cystic fibrosis lung and human gut. Gut Microbes 1:85–93.

50. Green HD, Jones AM. 2022. Managing Pulmonary Infection in Adults With Cystic Fibrosis: Adult Cystic Fibrosis Series. Chest. Elsevier Inc. https://doi.org/10.1016/j.chest.2022.02.007.

51. Beghini F, McIver LJ, Blanco-Míguez A, Dubois L, Asnicar F, Maharjan S, Mailyan A, Manghi P, Scholz M, Thomas AM, Valles-Colomer M, Weingart G, Zhang Y, Zolfo M, Huttenhower C, Franzosa EA, Segata N. 2021. Integrating taxonomic, functional, and strain-level profiling of diverse microbial communities with biobakery 3. Elife 10.

52. Mall MA, Brugha R, Gartner S, Legg J, Moeller A, Mondejar-Lopez P, Prais D, Pressler T, Ratjen F, Reix P, Robinson PD, Selvadurai H, Stehling F, Ahluwalia N, Arteaga-Solis E, Bruinsma BG, Jennings M, Moskowitz SM, Noel S, Tian S, Weinstock TG, Wu P, Wainwright CE, Davies JC. 2022. Efficacy and Safety of Elexacaftor/Tezacaftor/Ivacaftor in Children 6 Through 11 Years of Age with Cystic Fibrosis Heterozygous for F508del and a Minimal Function Mutation A Phase 3b, Randomized, Placebo-controlled Study. Am J Respir Crit Care Med 206:1361–1369.

53. Streibel C, Willers CC, Pusterla O, Bauman G, Stranzinger E, Brabandt B, Bieri O, Curdy M, Bullo M, Frauchiger BS, Korten I, Krüger L, Casaulta C, Ratjen F, Latzin P, Kieninger E. 2023. Effects of elexacaftor/tezacaftor/ivacaftor therapy in children with cystic fibrosis – a comprehensive assessment using lung clearance index, spirometry, and functional and structural lung MRI. Journal of Cystic Fibrosis https://doi.org/10.1016/j.jcf.2022.12.012.

54. Jordan KD, Zemanick ET, Taylor-Cousar JL, Hoppe JE. 2023. Managing cystic fibrosis in children aged 6-11yrs: a critical review of elexacaftor/tezacaftor/ivacaftor combination therapy. Expert Rev Respir Med. Taylor and Francis Ltd. https://doi.org/10.1080/17476348.2023.2179989.

55. Kapouni N, Moustaki M, Douros K, Loukou I. 2023. Efficacy and Safety of Elexacaftor-Tezacaftor-Ivacaftor in the Treatment of Cystic Fibrosis: A Systematic Review. Children 10:554.

56. Wainwright C, McColley SA, McNally P, Powers M, Ratjen F, Rayment JH, Retsch-Bogart G, Roesch E, Ahluwalia N, Chin A, Chu C, Lu M, Menon P, Waltz D, Weinstock T, Zelazoski L, Davies JC, VX19-445-107 Study Group. 2023. Long-Term Safety and Efficacy of Elexacaftor/Tezacaftor/Ivacaftor in Children Aged ≥6 Years with Cystic

Fibrosis and At Least One F508del Allele: A Phase 3, Open-Label Clinical Trial. Am J Respir Crit Care Med https://doi.org/10.1164/rccm.202301-0021OC.

57. Cornet M, Robin G, Ciciriello F, Bihouee T, Marguet C, Roy V, Lebourgeois M, Chedevergne F, Bonnel AS, Kelly M, Reix P, Lucidi V, Stoven V, Sermet-Gaudelus I. 2022. Profiling the response to lumacaftor-ivacaftor in children with cystic between fibrosis and new insight from a French-Italian real-life cohort. Pediatr Pulmonol https://doi.org/10.1002/ppul.26123.
58. Appelt D, Steinkamp G, Sieber S, Ellemunter H. 2023. Early and sustained improvements of lung clearance index from two to sixteen weeks of elexacaftor/tezacaftor/ivacaftor therapy in patients with cystic fibrosis—a real world study. Front Pharmacol 14.
59. Gramegna A, Majo F, Alicandro G, Leonardi G, Cristiani L, Amati F, Contarini M, Aliberti S, Fiocchi AG, Blasi F. 2023. Heterogeneity of weight gain after initiation of Elexacaftor/Tezacaftor/Ivacaftor in people with cystic fibrosis. Respir Res 24.
60. Matamouros S, Hayden HS, Hager KR, Brittnacher MJ, Lachance K, Weiss EJ, Pope CE, Imhaus AF, McNally CP, Borenstein E, Hoffman LR, Miller SI. 2018. Adaptation of commensal proliferating Escherichia coli to the intestinal tract of young children with cystic fibrosis. Proc Natl Acad Sci U S A 115:1605–1610.
61. Freitas MB De, Addison E, Moreira M, Tomio C, Maria Y, Moreno F, Daltoe FP, Barbosa E, Neto NL, Buccigrossi V, Guarino A. 2018. Altered intestinal microbiota composition, antibiotic therapy and intestinal inflammation in children and adolescents with cystic fibrosis. PLoS One 13.
62. Duytschaever G, Huys G, Bekaert M, Boulanger L, De Boeck K, Vandamme P. 2013. Dysbiosis of bifidobacteria and Clostridium cluster XIVa in the cystic fibrosis fecal microbiota. Journal of Cystic Fibrosis 12:206–215.
63. Nielsen S, Needham B, Leach ST, Day AS, Jaffe A, Thomas T, Ooi CY. 2016. Disrupted progression of the intestinal microbiota with age in children with cystic fibrosis. Sci Rep 6.
64. Debyser G, Mesuere B, Clement L, Van de Weygaert J, Van Hecke P, Duytschaever G, Aerts M, Dawyndt P, De Boeck K, Vandamme P, Devreese B. 2016. Faecal proteomics: A tool to investigate dysbiosis and inflammation in patients with cystic fibrosis. Journal of Cystic Fibrosis 15:242–250.
65. Bernard R, Shilts MH, Strickland BA, Boone HH, Payne DC, Brown RF, Edwards K, Das SR, Nicholson MR. 2023. The relationship between the intestinal microbiome and body mass index in children with cystic fibrosis. Journal of Cystic Fibrosis https://doi.org/10.1016/j.jcf.2023.11.002.
66. Hollister EB, Riehle K, Luna RA, Weidler EM, Rubio-Gonzales M, Mistretta TA, Raza S, Doddapaneni H V., Metcalf GA, Muzny DM, Gibbs RA, Petrosino JF, Shulman RJ, Versalovic J. 2015. Structure and function of the healthy pre-adolescent pediatric gut microbiome. Microbiome 3:36.
67. Mehta RS, Abu-Ali GS, Drew DA, Lloyd-Price J, Subramanian A, Lochhead P, Joshi AD, Ivey KL, Khalili H, Brown GT, Dulong C, Song M, Nguyen LH, Mallick H, Rimm EB, Izard J, Huttenhower C, Chan AT. 2018. Stability of the human faecal microbiome in a cohort of adult men. Nat Microbiol 3:347–355.
68. David LA, Materna AC, Friedman J, Campos-Baptista MI, Blackburn MC, Perrotta A, Erdman SE, Alm EJ. 2014. Host lifestyle affects human microbiota on daily timescales. Genome Biol 15.

69. Faith JJ, Guruge JL, Charbonneau M, Subramanian S, Seedorf H, Goodman AL, Clemente JC, Knight R, Heath AC, Leibel RL, Rosenbaum M, Gordon JI. 2013. The long-term stability of the human gut microbiota. Science (1979) 341.
70. Yamada A, Komaki Y, Komaki F, Micic D, Zullow S, Sakuraba A. 2018. Risk of gastrointestinal cancers in patients with cystic fibrosis: a systematic review and meta-analysis. Lancet Oncol 19:758–767.
71. Garg M, Leach ST, Coffey MJ, Katz T, Strachan R, Pang T, Needham B, Lui K, Ali F, Day AS, Appleton L, Moeeni V, Jaffe A, Ooi CY. 2017. Age-dependent variation of fecal calprotectin in cystic fibrosis and healthy children. Journal of Cystic Fibrosis 16:631–636.
72. Rumman N, Sultan M, El-Chammas K, Goh V, Salzman N, Quintero D, Werlin S. 2014. Calprotectin in Cystic Fibrosis. BMC Pediatr 14.
73. Beaufils F, Mas E, Mittaine M, Addra M, Fayon M, Delhaes L, Clouzeau H, Galode F, Lamireau T, Bui S, Enaud R. 2020. Increased Fecal Calprotectin Is Associated with Worse Gastrointestinal Symptoms and Quality of Life Scores in Children with Cystic Fibrosis. J Clin Med 9:4080.
74. Schwarzenberg SJ, Vu PT, Skalland M, Hoffman LR, Pope C, Gelfond D, Narkewicz MR, Nichols DP, Heltshe SL, Donaldson SH, Frederick CA, Kelly A, Pittman JE, Ratjen F, Rosenfeld M, Sagel SD, Solomon GM, Stalvey MS, Clancy JP, Rowe SM, Freedman SD. 2022. Elexacaftor/tezacaftor/ivacaftor and gastrointestinal outcomes in cystic fibrosis: Report of promise-GI. Journal of Cystic Fibrosis https://doi.org/10.1016/j.jcf.2022.10.003.
75. Mainz JG, Lester K, Elnazir B, Williamson M, McKone E, Cox D, Linnane B, Zagoya C, Duckstein F, Barucha A, Davies JC, McNally P. 2023. Reduction in abdominal symptoms (CFAbd-Score), faecal M2-pyruvate-kinase and Calprotectin over one year of treatment with Elexacaftor-Tezacaftor-Ivacaftor in people with CF aged ≥12 years – The RECOVER study. Journal of Cystic Fibrosis https://doi.org/10.1016/j.jcf.2023.10.001.
76. Baldwin-Hunter BL, Rozenberg FD, Annavajhala MK, Park H, DiMango EA, Keating CL, Uhlemann A-C, Abrams JA. 2023. The gut microbiome, short chain fatty acids, and related metabolites in cystic fibrosis patients with and without colonic adenomas. Journal of Cystic Fibrosis https://doi.org/10.1016/j.jcf.2023.01.013.
77. Miragoli F, Federici S, Ferrari S, Minuti A, Rebecchi A, Bruzzese E, Buccigrossi V, Guarino A, Callegari ML. 2017. Impact of cystic fibrosis disease on archaea and bacteria composition of gut microbiota. FEMS Microbiol Ecol 93.
78. Burke DG, Fouhy F, Harrison MJ, Rea MC, Cotter PD, O'Sullivan O, Stanton C, Hill C, Shanahan F, Plant BJ, Ross RP. 2017. The altered gut microbiota in adults with cystic fibrosis. BMC Microbiol 17:1–11.
79. Rivera-Chávez F, Lopez CA, Bäumler AJ. 2017. Oxygen as a driver of gut dysbiosis. Free Radic Biol Med. Elsevier Inc. https://doi.org/10.1016/j.freeradbiomed.2016.09.022.
80. Shah YM. 2016. The role of hypoxia in intestinal inflammation. Mol Cell Pediatr 3.
81. Rigottier-Gois L. 2013. Dysbiosis in inflammatory bowel diseases: The oxygen hypothesis. ISME Journal https://doi.org/10.1038/ismej.2013.80.
82. López-Causapé C, Rojo-Molinero E, MacIà MD, Oliver A. 2015. The problems of antibiotic resistance in cystic fibrosis and solutions. Expert Rev Respir Med. Expert Reviews Ltd. https://doi.org/10.1586/17476348.2015.995640.
83. Taylor SL, Leong LEX, Sims SK, Keating RL, Papanicolas LE, Richard A, Mobegi FM, Wesselingh S, Burr LD, Rogers GB. 2021. The cystic fibrosis gut as a potential source of multidrug resistant pathogens. Journal of Cystic Fibrosis 20:413–420.

84. Fredriksen S, de Warle S, van Baarlen P, Boekhorst J, Wells JM. 2023. Resistome expansion in disease-associated human gut microbiomes. Microbiome 11:166.
85. Patel D, Mathews S, van Unen V, Chan JE, Al-Hammadi N, Borowitz D, Gelfond D, Sellers ZM. 2022. Impaired distal colonic pH in adults with cystic fibrosis. Journal of Cystic Fibrosis https://doi.org/10.1016/j.jcf.2022.12.011.
86. Gelfond D, Heltshe S, Ma C, Rowe SM, Frederick C, Uluer A, Sicilian L, Konstan M, Tullis E, Roach RNC, Griffin K, Joseloff E, Borowitz D. 2017. Impact of CFTR modulation on intestinal pH, motility, and clinical outcomes in patients with cystic fibrosis and the G551D mutation. Clin Transl Gastroenterol 8.

TABLES AND FIGURES

Supplementary Table S10. Stratified Taxonomic Output of Differentially Abundant KEGG Orthology Groups

Supplementary Dataset 1. Compiled Metadata and Metagenomic Results

FIGURE LEGENDS

Figure 1. Study Schematic, Timeline, and Clinical Improvement after ELX/TEZ/IVA. **A)** Overview of study procedure and analyses. **B)** Timeline illustrating the four timepoints. Day 0 is depicted as the day of ELX/TEZ/IVA initiation. A total of 114 samples were collected from 39 unique patients, of which 53 samples were before ELX/TEZ/IVA treatment and 61 samples after treatment. **C-E)** Depictions of clinical data before and after ELX/TEZ/IVA; **(C)** ppFEV1, **(D)** BMI percentile, **(E)** antibiotic days per 6-months. Each dot represents the clinical data associated with a stool sample. P values calculated by Wilcoxon rank-sum test.

Figure 2. Microbiome Diversity and Intestinal Carriage of Antibiotic Resistance Genes. **A)** Phylum level relative abundance for samples collected before (samples=53) and after (samples=61) ELX/TEZ/IVA. Samples are organized by the relative abundance of the phylum Firmicutes. **B-C)** Alpha diversity before and after ELX/TEZ/IVA. Shannon Index calculated with the R package vegan using species abundance table from Metaphlan4. Microbial richness represents the number of unique species per sample. Each dot represents a stool sample (samples=114). P values calculated by Wilcoxon rank-sum test. **D-E)** Alpha diversity between samples with and without recent antibiotic exposure. Recent antibiotic exposure categorized as any systemic antibiotic within the past 6-months. Shannon Index calculated with the R package vegan using species abundance table from MetaPhlAn4. Microbial richness represents the number of unique species per sample. Each dot represents a stool sample (samples=114). P values calculated by Wilcoxon rank-sum test.

Figure 3. A) Antibiotic resistance gene **(**ARG) abundance (RPKM) before and after ELX/TEZ/IVA. ARGs were profiled using ShortBRED and the Comprehensive Antibiotic Resistance Database (CARD). Each dot represents a stool sample (samples=114). P values calculated by Wilcoxon rank-sum test. **B)** ARG abundance (RPKM) by class of antibiotic to which they confer resistance. Abundance values of zero are plotted on the vertical axis. P values calculated by Wilcoxon signed-rank test.

Figure 4. Specific Microbial Taxonomic Changes after ELX/TEZ/IVA.
A) Differentially abundant species before and after ELX/TEZ/IVA. The results are depicted with significance (−log10 of the FDR) (Y axis) vs. log2(FoldChange). MaAsLin2 multivariable association modeling was implemented in R, using ELX/TEZ/IVA status, age, and recent antibiotics as fixed effects in the model. Participant ID was used as a random effect. Horizontal dashed line depicts FDR=0.1. Species reaching statistical significance (FDR≤0.10) are highlighted in solid colors whereas other species are gray. **B)** Species of interest from differential abundance testing before and after ELX/TEZ/IVA. Vertical axis is log10 transformed. MaAsLin2 FDR is depicted. Zero values are plotted on the horizontal axes. The percentage of samples for which the relative abundance was zero is depicted below the graph.

Figure 5. Intestinal Inflammation Decreases after ELX/TEZ/IVA and Microbiome Functional Changes. A) Fecal calprotectin before and after ELX/TEZ/IVA. Each dot represents a stool sample (samples=114). P values calculated by Wilcoxon rank-sum test. **B-C)** Microbial dysbiosis index (MD-INDEX) before and after ELX/TEZ/IVA **(B)** or between samples with and without recent antibiotic exposure **(C)**. MD-index calculated as the log10 ratio of species positively/negatively correlated with new onset pediatric Crohn's disease (44). Each dot represents a stool sample (samples=114). P values calculated by Wilcoxon rank-sum test. **D)** Differentially abundant KEGG orthologs following MaAsLin2 multivariable association modeling, using ELX/TEZ/IVA status, age, and recent antibiotics as fixed effects in the model. Participant ID was used as a random effect. Horizontal dashed line depicts FDR=0.25. **E)** Subset of differentially abundant MetaCyc pathways following MaAsLin2 multivariable association modeling, using ELX/TEZ/IVA status, age, and recent antibiotics as fixed effects in the model. Only pathways with FDR<0.25 are depicted.

Supplementary Figure S1. A-D) Clinical metadata vs. timepoint; **(A)** ppFEV1, **(B)** BMI percentile, **(C)** weight percentile, and **(D)** height percentile. Each dot represents the clinical data associated with a stool sample. Red line indicates the mean, and gray lines represent individual patients. P values calculated by Wilcoxon signed-rank test.

Supplementary Figure S2. A-B) Alpha diversity vs. timepoint. Shannon Index (**A**) calculated with the R package vegan using species abundance table from Metaphlan4. Microbial richness (**B**) represents the number of unique species per sample. Each dot represents a stool sample (samples=114). P values calculated by Wilcoxon signed-rank test. **C)** Principal component

analysis of Bray-Curtis distances before and after ELX/TEZ/IVA. Bray-Curtis distance matrix computed with vegan. PERMANOVA and PERMDISP computed by the vegan package with the functions adonis2 and betadisp, respectively. Ellipse depicts the 95% confidence level. **D)** Principal component analysis of weighted UniFrac distances before and after ELX/TEZ/IVA. Weighted UniFrac computed with MetaPhlAn4 R script. PERMANOVA and PERMDISP computed by the vegan package with the functions adonis2 and betadisp, respectively. Ellipse depicts the 95% confidence level. **E)** Principal component analysis of the Bray-Curtis distances between samples with and without recent antibiotic exposure. Distance matrix generated by the R package vegan using the MetaPhlAn4 species table. PERMANOVA and PERMDISP computed in vegan with the functions adonis2 and betadisp, respectively. Ellipse depicts the 95% confidence level.

Supplementary Figure S3. A-B) Diversity metrics of pre-ELX/TEZ/IVA samples (samples=53 total). Samples are grouped by whether the subject was receiving another CFTR modulator at the time of sample collection (Yes=8, No=45). **C-D)** Diversity metrics of pre-ELX/TEZ/IVA samples (samples=53) compared to post-ELX/TEZ/IVA samples (samples=61). Post-ELX/TEZ/IVA samples were segregated by whether the subject had previously received any other CFTR modulator (Yes=20 samples, No=41 samples). Shannon Index calculated with the R package vegan using species abundance table from MetaPhlAn4. Microbial richness represents the number of unique species per sample. P values calculated by Wilcoxon rank-sum test.

Supplementary Figure S4. A) Cumulative antibiotic days per 6-months prior to stool sample collection. P values calculated by Wilcoxon signed-rank test. **B)** ARG richness (unique genes) before and after ELX/TEZ/IVA. ARGs were profiled using ShortBRED and the Comprehensive Antibiotic Resistance Database (CARD). Each dot represents a stool sample (samples=114). P values calculated by Wilcoxon rank-sum test. **C)** Cumulative relative abundance (RPKM) of ARGs conferring resistance to peptide antibiotics. P values calculated by Wilcoxon rank-sum test. **D)** Relative abundance (RPKM) of the most prevalent ARGs conferring resistance to peptide antibiotics. MaAsLin2 FDR is depicted. **E)** Cumulative relative abundance (RPKM) of ARGs conferring resistance to other antibiotics. P values calculated by Wilcoxon rank-sum test. **F)** Relative abundance (RPKM) of the most prevalent ARGs conferring resistance to other antibiotics. MaAsLin2 FDR is depicted.

Supplementary Figure S5. A) *Roseburia faecis* relative abundance between samples with and without recent antibiotic exposure. Each dot represents a stool sample (samples=114). MaAsLin2 FDR is depicted. **B)** Relative abundance of respiratory genera in stool samples before and after ELX/TEZ/IVA. Each dot represents a stool sample (samples=114). MaAsLin2 FDR is depicted. Vertical axis is log10 transformed. Zero values are plotted on the horizontal axes.

Supplementary Figure S6. A) Fecal calprotectin (µg/g) vs. study timepoint. Red line indicates the mean, and gray lines represent individual patients. P values calculated by Wilcoxon signed-rank test. **B)** Differentially abundant oxidative phosphorylation KEGG orthology (KO) groups from MaAsLin2 (FDR<0.25). Groups correspond to red points in Fig. 5A. log2(FoldChange), which is equivalent to MaAsLin2 coefficient, is depicted. **C)** Taxonomic stratification of differentially abundant oxidative phosphorylation KO groups. KO groups correspond to groups in panel A.

Supplementary Figure S7. Differentially abundant MetaCyc pathways following MaAsLin2 multivariable association modeling, using ELX/TEZ/IVA status, age, and recent antibiotics as fixed effects in the model. Only pathways with FDR<0.25 are depicted.

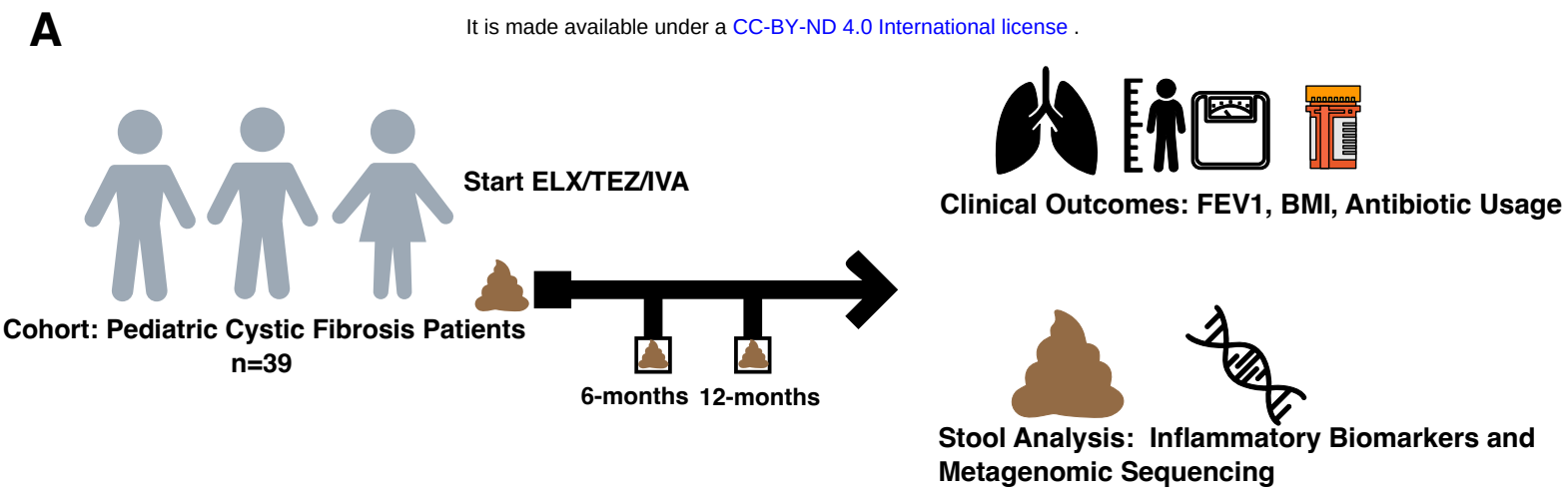

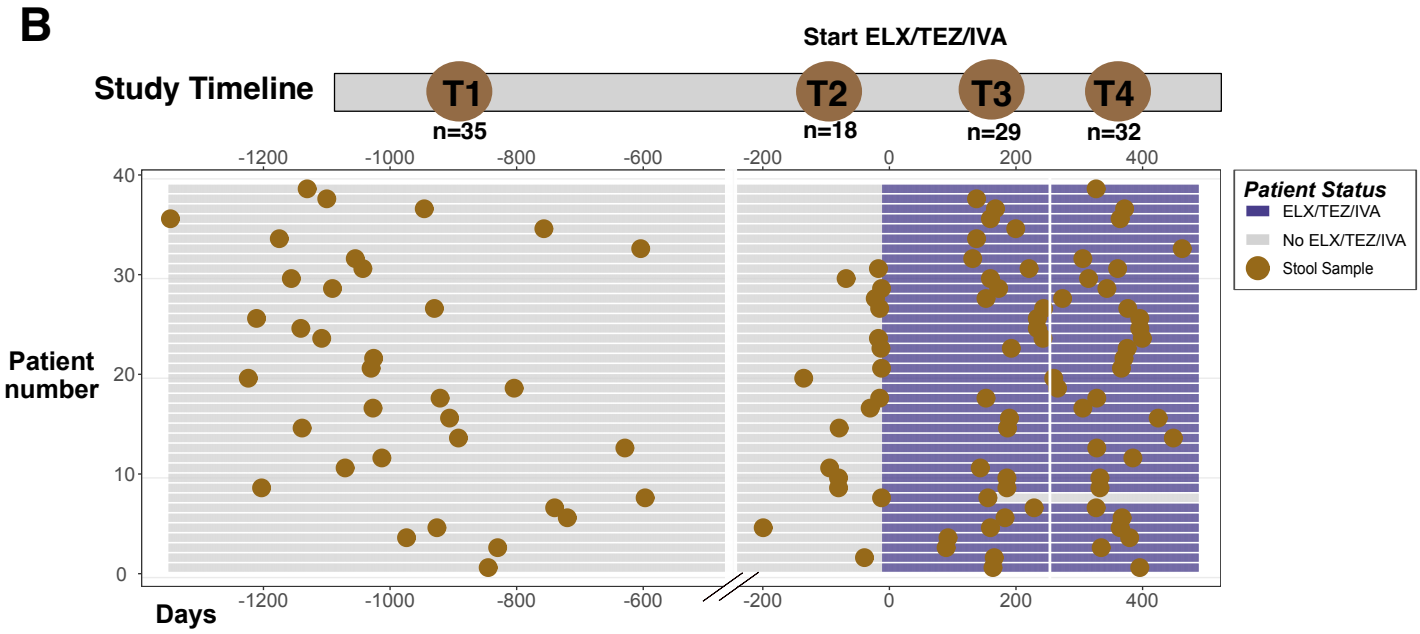

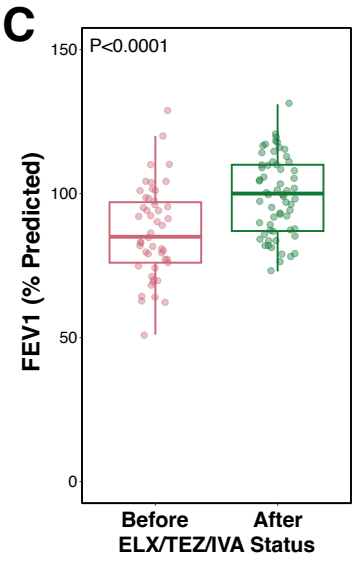

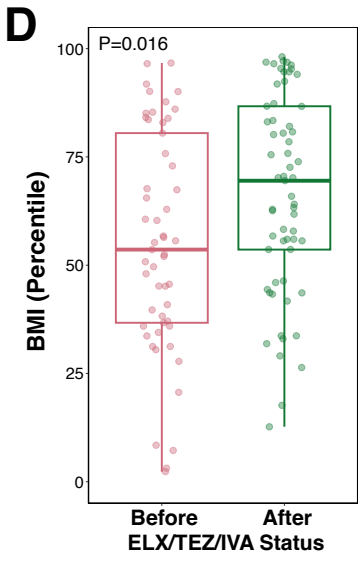

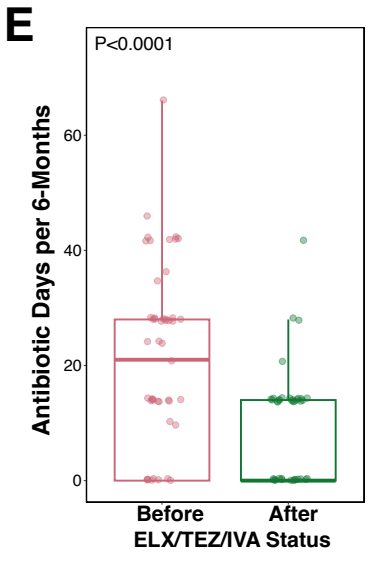

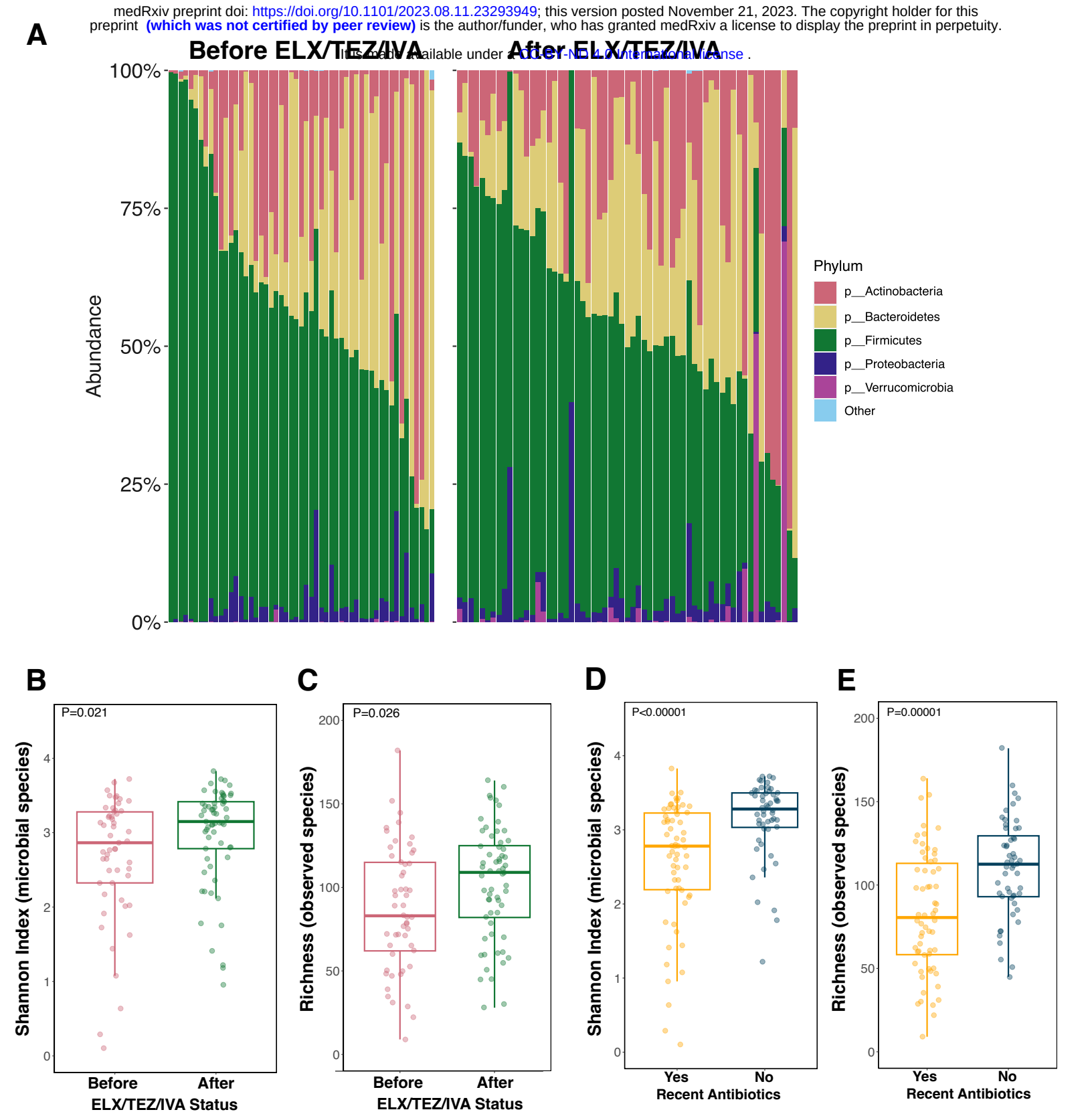

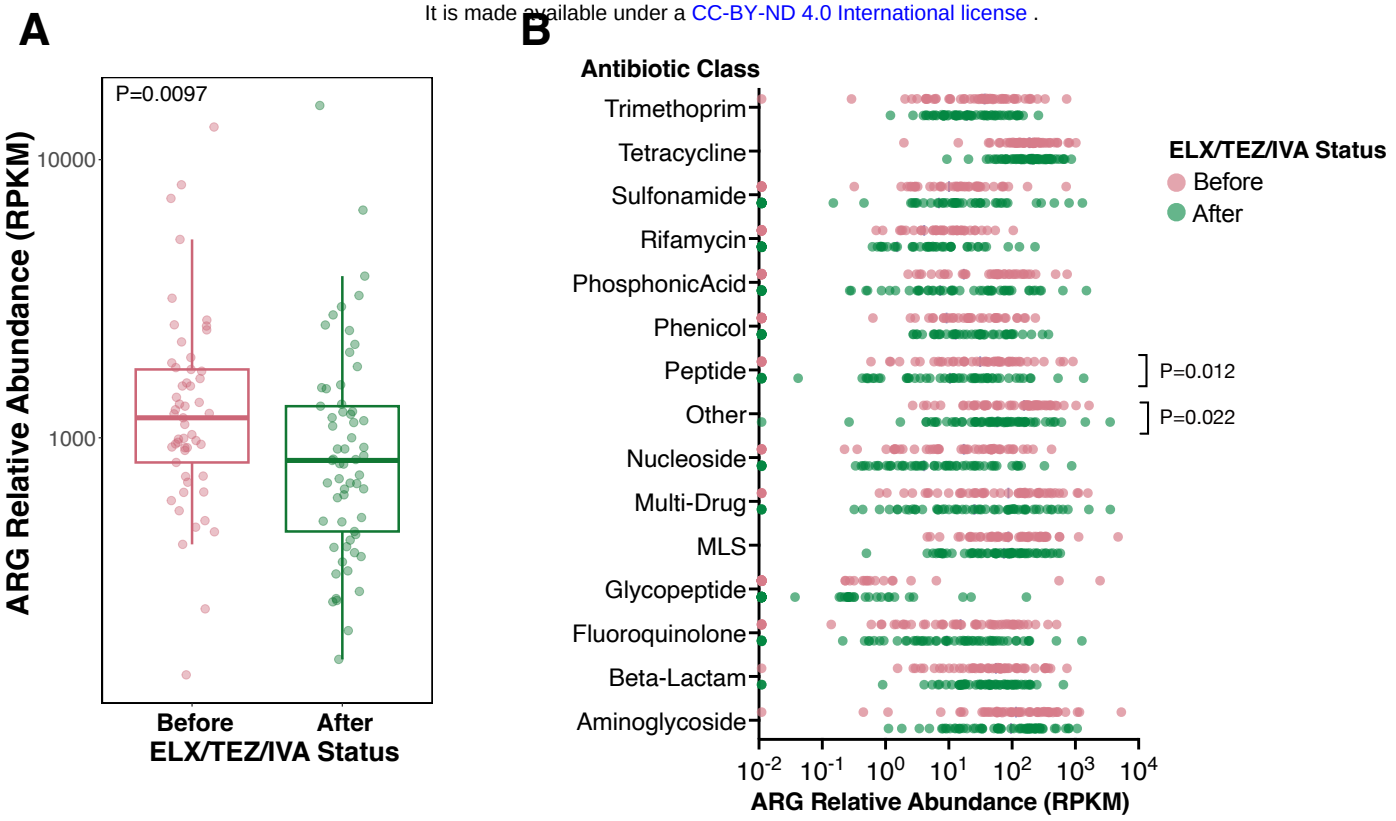

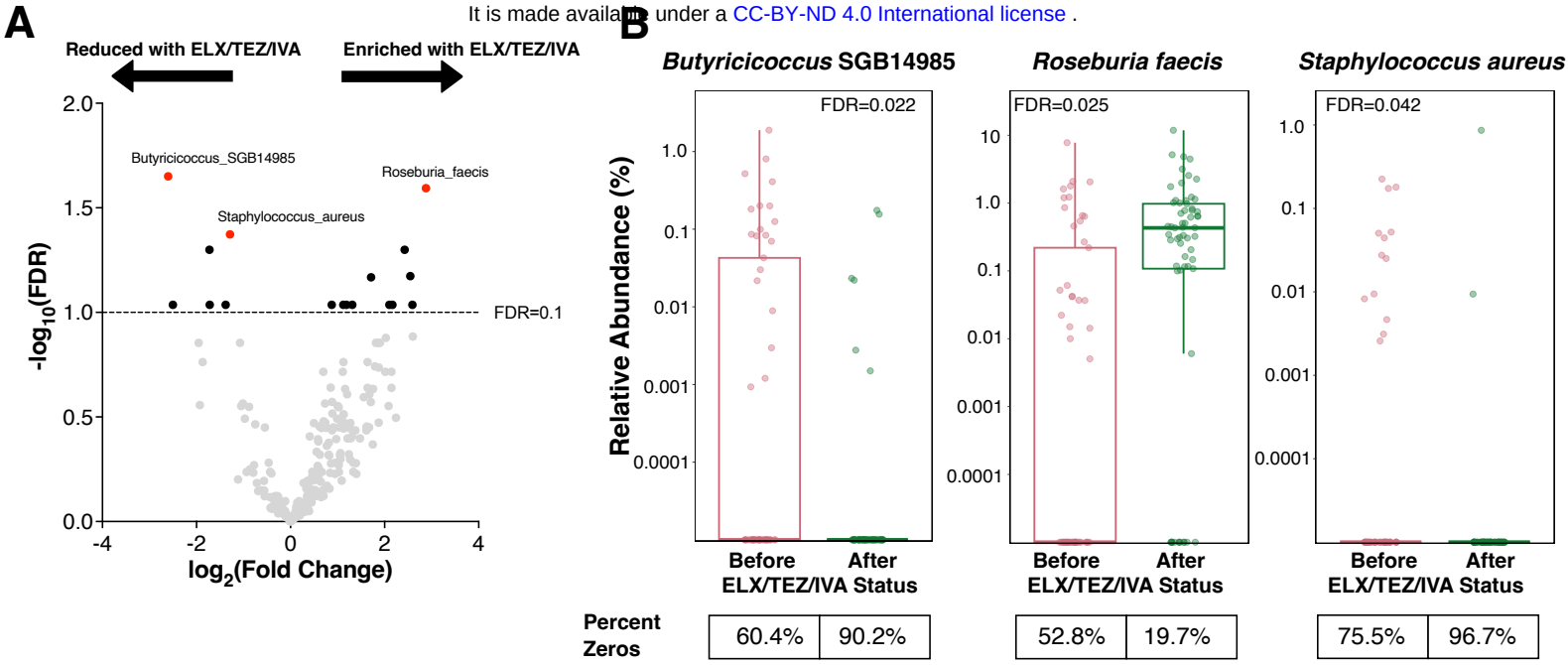

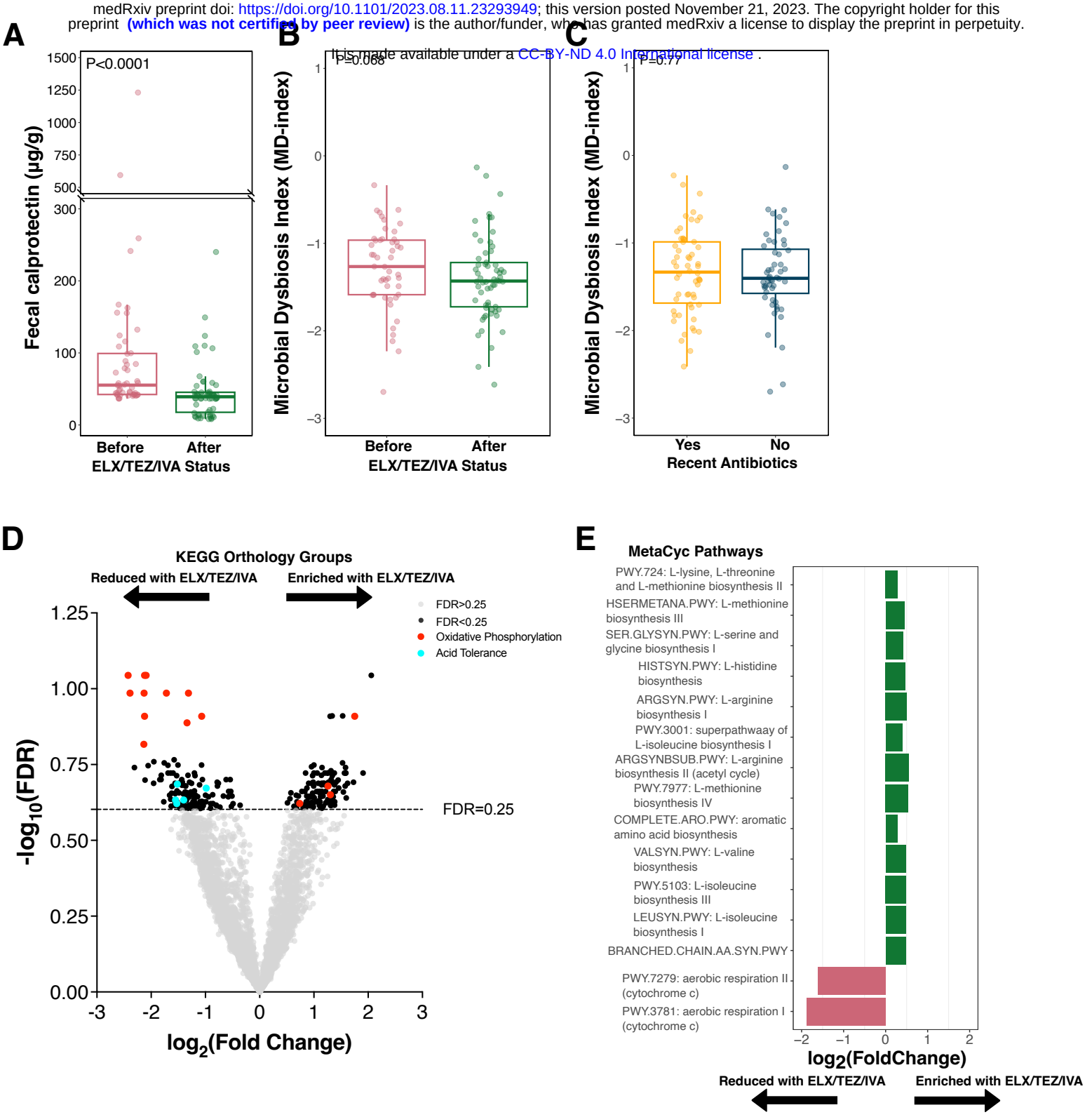

Supplemental Figure 1

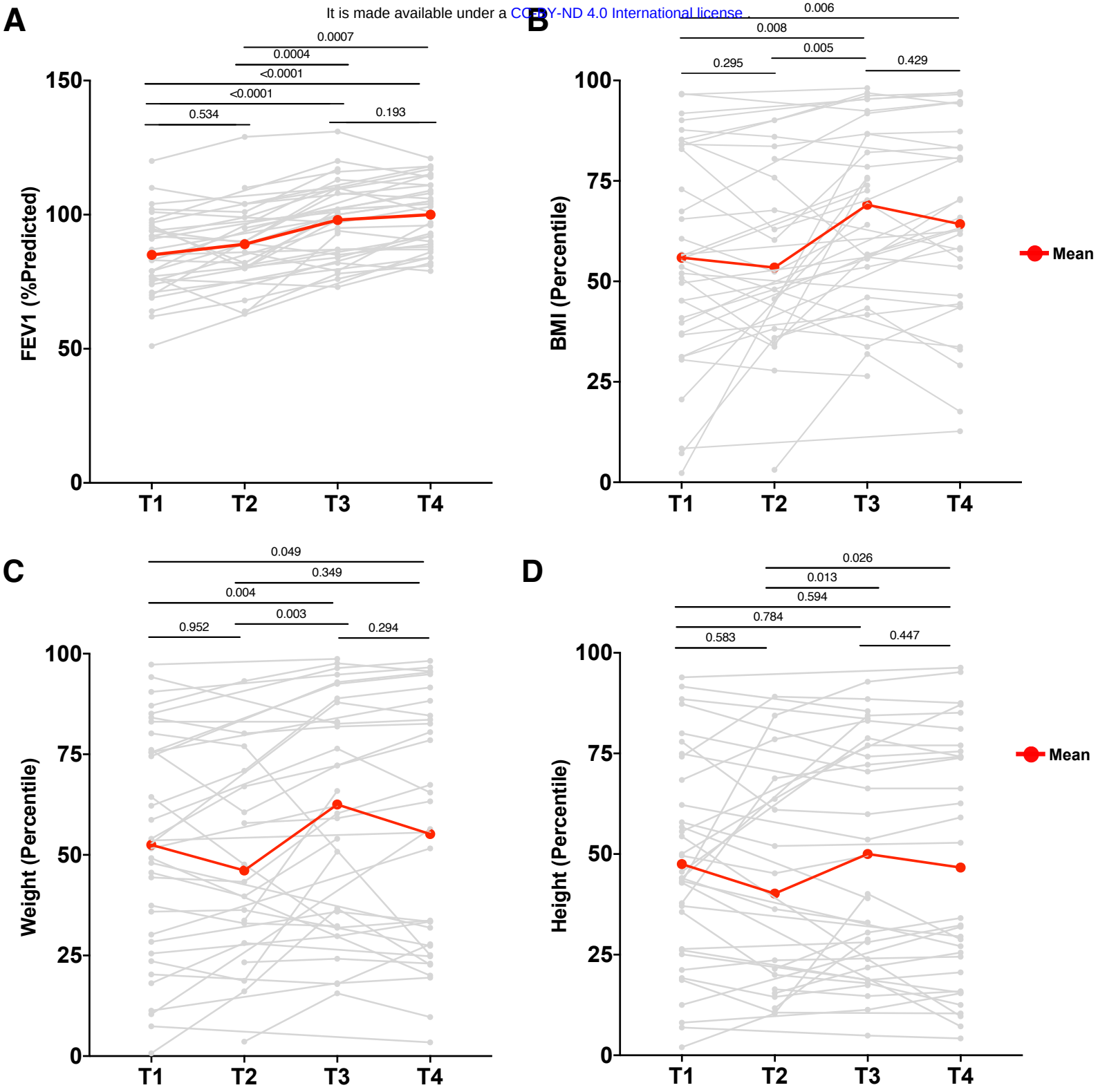

Supplemental Figure 2

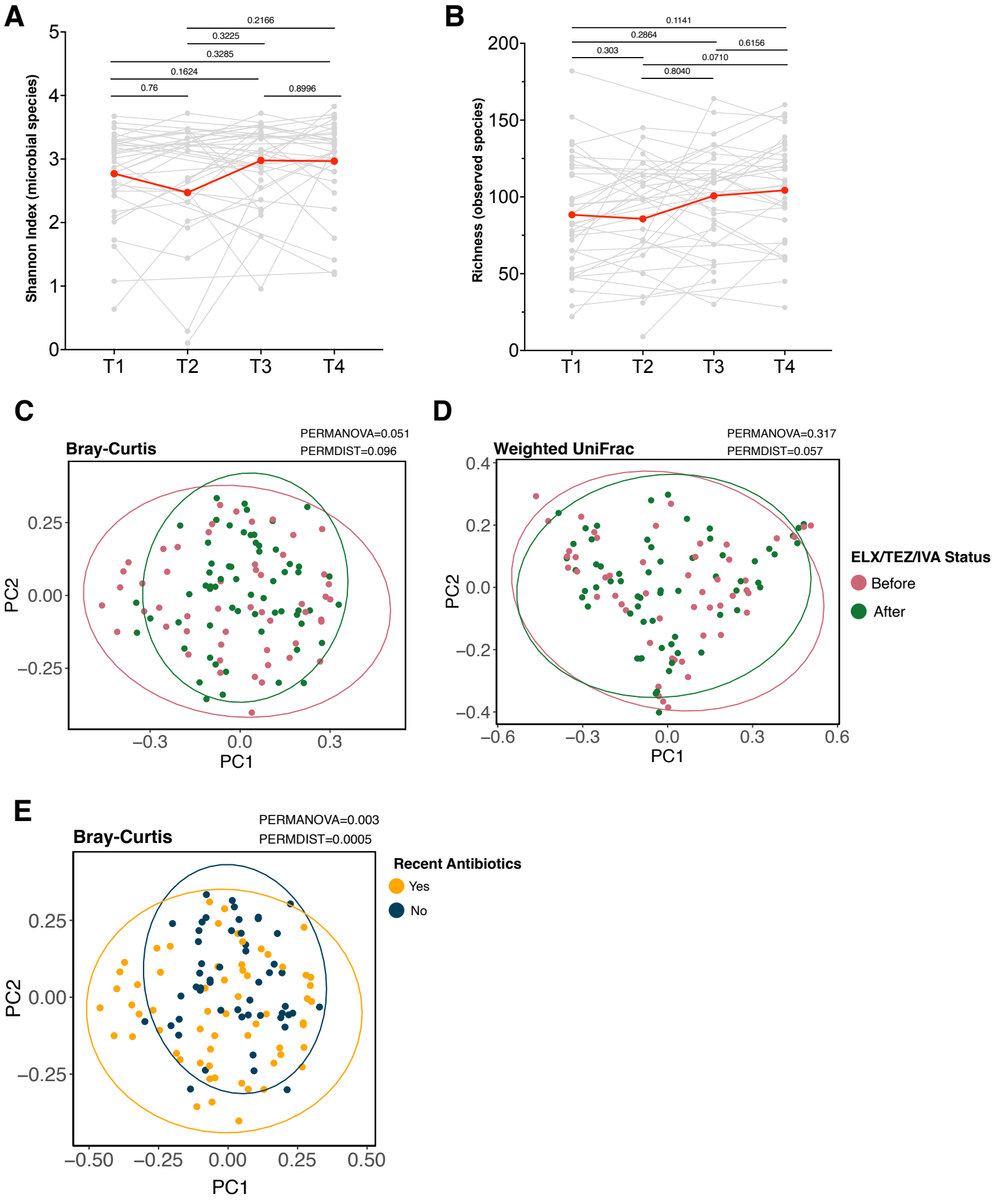

Supplemental Figure 3

Before ELX/TEZ/IVA

53 total samples
45 modulator naïve samples
8 samples on another modulator

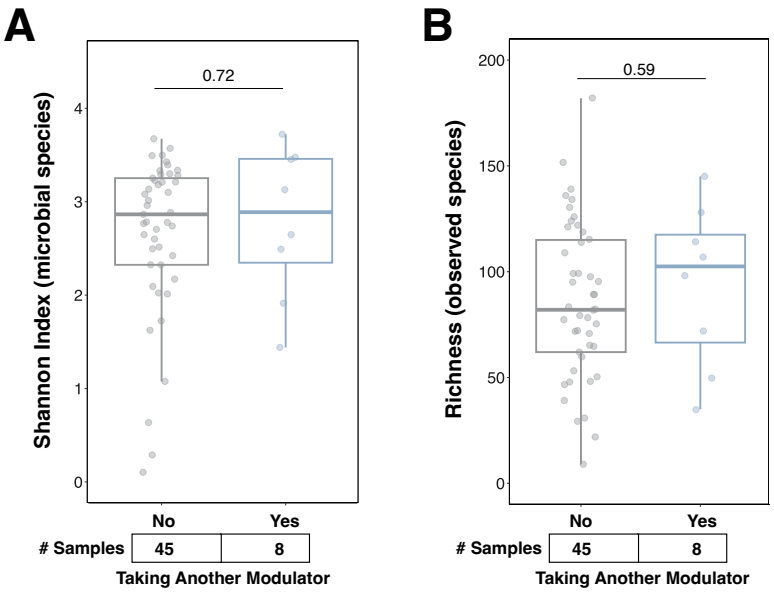

After ELX/TEZ/IVA

61 total samples
41 samples from subjects without prior modulator use
20 samples from subjects with prior modulator use

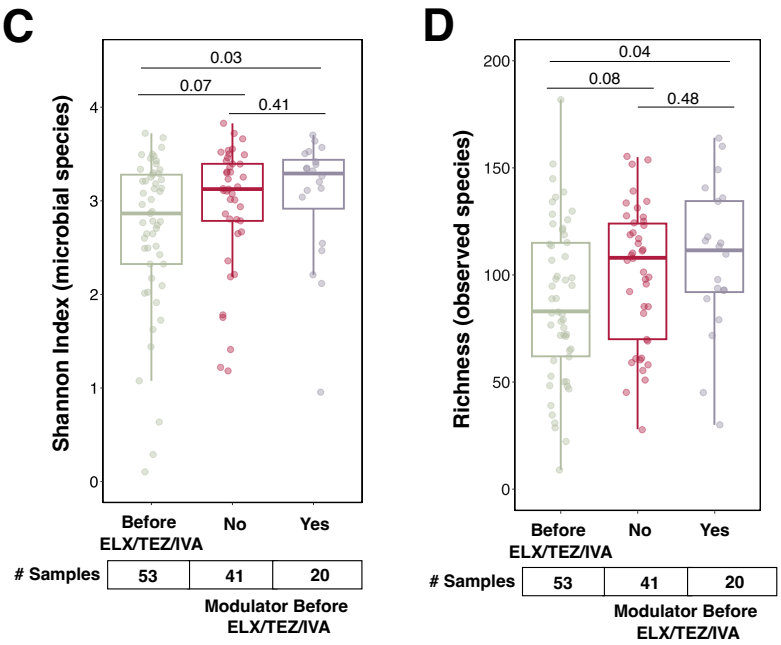

Supplemental Figure 4

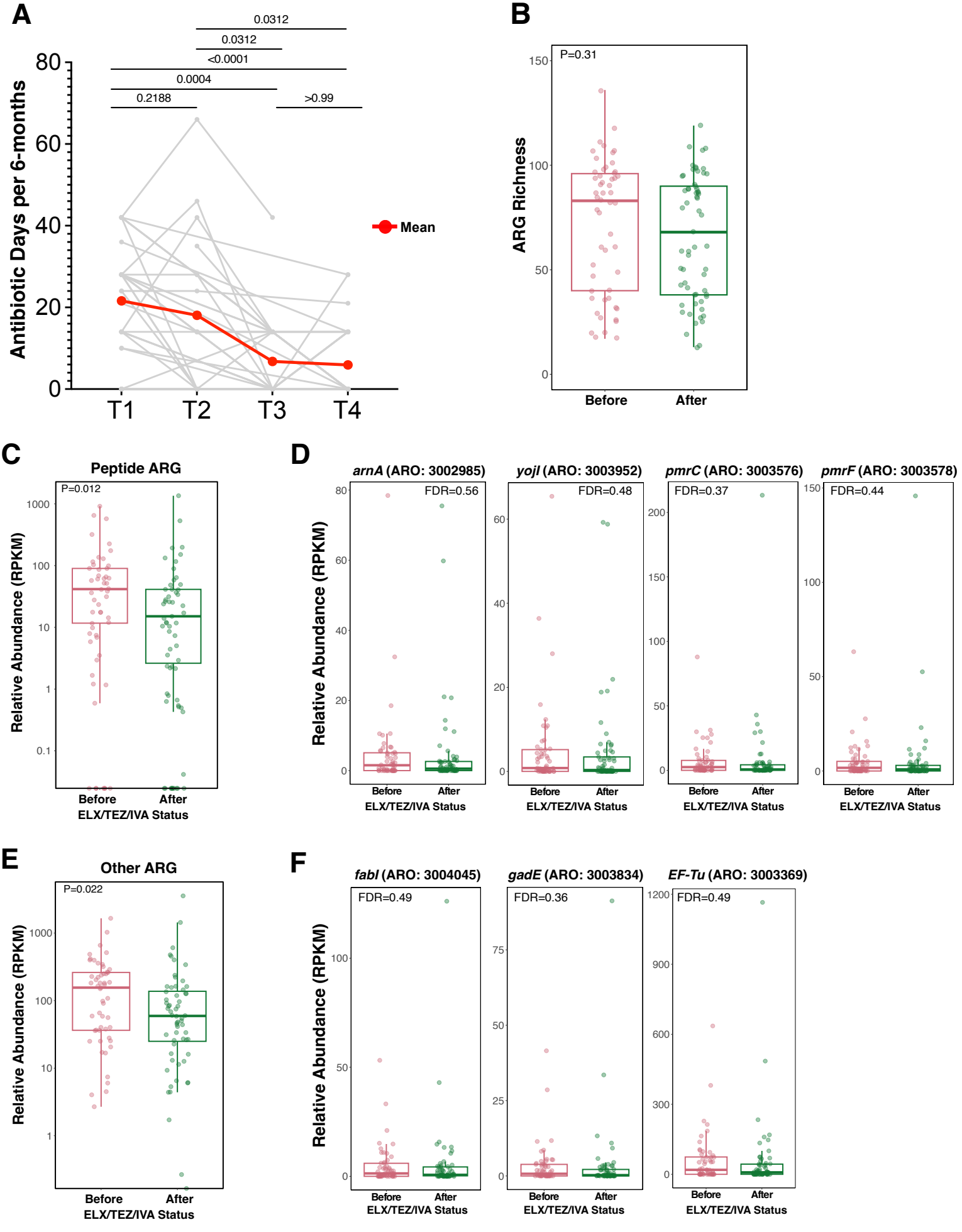

Supplemental Figure 5

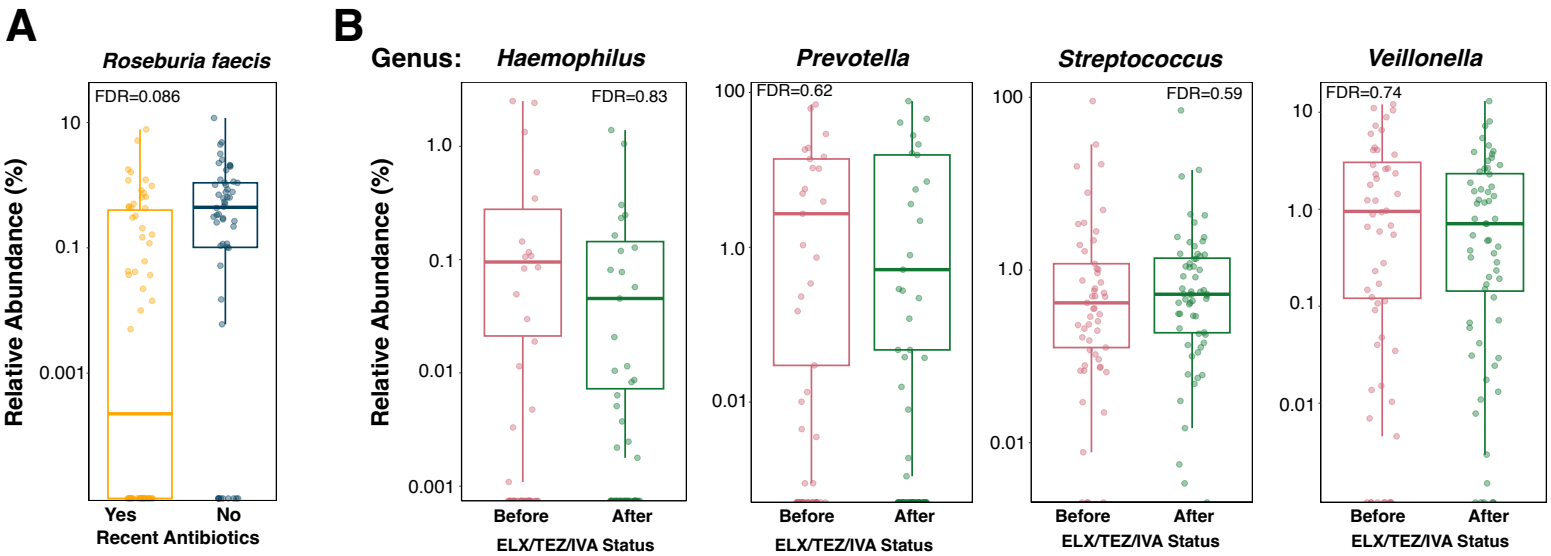

Supplemental Figure 6

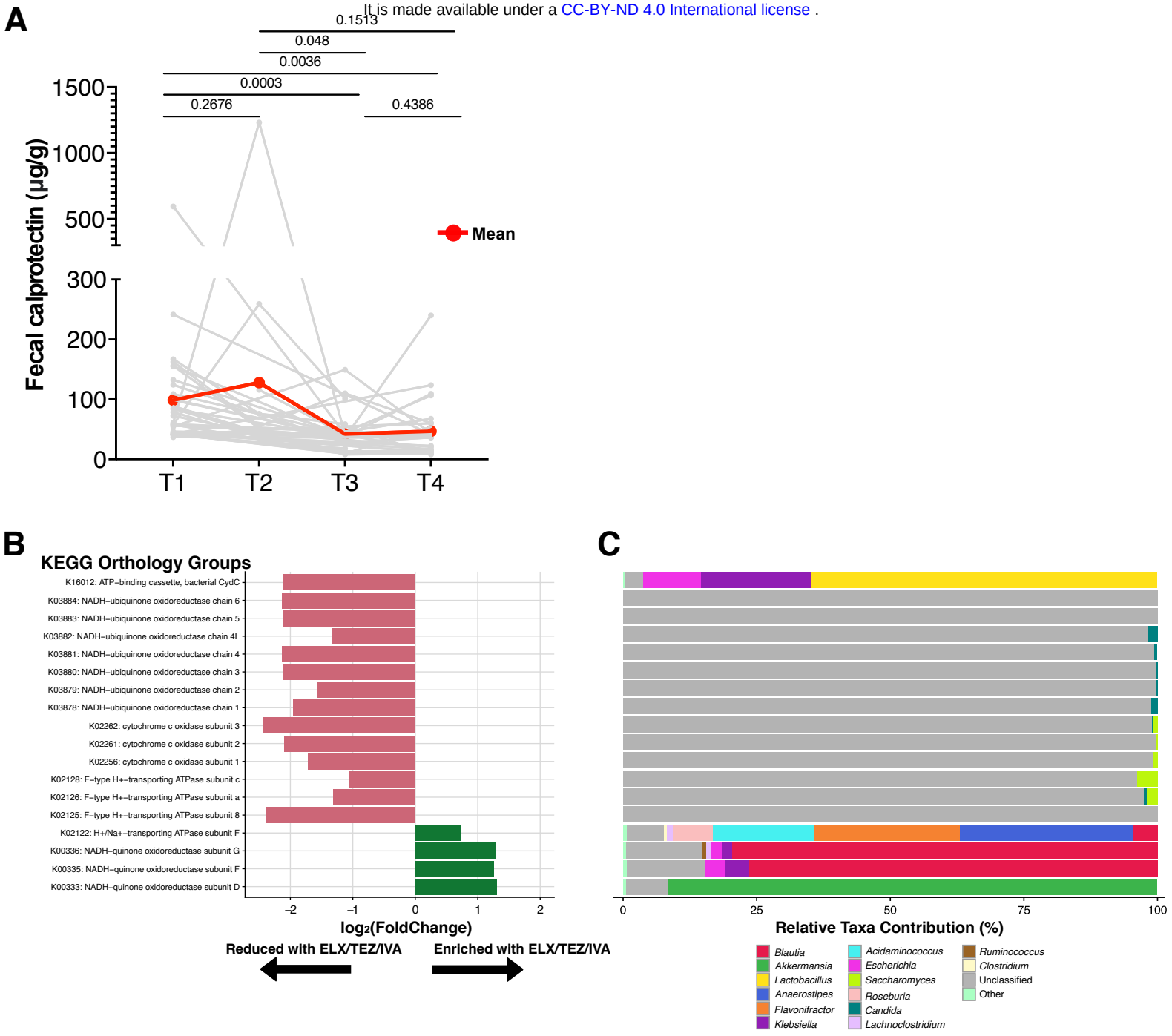

Supplemental Figure 7